

AFRL-AFOSR-UK-TR-2011-0016



**The Nature of the Microstructure and Interface Boundary
Formation in Directionally Solidified Ceramic Boride
Composites**

Volodymyr B Filipov

**Frantsevich Institute for Problems in Materials Science NAS of
Ukraine**

REE Refractory Compounds Laboratory

3 Krzhyzhanovskyy Street

Kiev, Ukraine 03142

EOARD STCU 06-8010

May 2011

Final Report for 12 June 2007 to 12 June 2010

Distribution Statement A: Approved for public release distribution is unlimited.

**Air Force Research Laboratory
Air Force Office of Scientific Research
European Office of Aerospace Research and Development
Unit 4515 Box 14, APO AE 09421**

REPORT DOCUMENTATION PAGE				Form Approved OMB No. 0704-0188	
<small>Public reporting burden for this collection of information is estimated to average 1 hour per response, including the time for reviewing instructions, searching existing data sources, gathering and maintaining the data needed, and completing and reviewing the collection of information. Send comments regarding this burden estimate or any other aspect of this collection of information, including suggestions for reducing the burden, to Department of Defense, Washington Headquarters Services, Directorate for Information Operations and Reports (0704-0188), 1215 Jefferson Davis Highway, Suite 1204, Arlington, VA 22202-4302. Respondents should be aware that notwithstanding any other provision of law, no person shall be subject to any penalty for failing to comply with a collection of information if it does not display a currently valid OMB control number.</small> PLEASE DO NOT RETURN YOUR FORM TO THE ABOVE ADDRESS.					
1. REPORT DATE (DD-MM-YYYY) 26-05-2011		2. REPORT TYPE Final Report		3. DATES COVERED (From – To) 12 June 2007 – 12 June 2010	
4. TITLE AND SUBTITLE The Nature of the Microstructure and Interface Boundary Formation in Directionally Solidified Ceramic Boride Composites			5a. CONTRACT NUMBER STCU Registration No: P-261		
			5b. GRANT NUMBER STCU 06-8010		
			5c. PROGRAM ELEMENT NUMBER		
6. AUTHOR(S) Volodymyr B. Filipov			5d. PROJECT NUMBER		
			5d. TASK NUMBER		
			5e. WORK UNIT NUMBER		
7. PERFORMING ORGANIZATION NAME(S) AND ADDRESS(ES) Frantsevich Institute for Problems in Materials Science NAS of Ukraine 3, Krzhyzhanovskyy Street Kiev, Ukraine 03142				8. PERFORMING ORGANIZATION REPORT NUMBER N/A	
9. SPONSORING/MONITORING AGENCY NAME(S) AND ADDRESS(ES) EOARD Unit 4515 BOX 14 APO AE 09421				10. SPONSOR/MONITOR'S ACRONYM(S) AFRL/AFOSR/RSW (EOARD)	
				11. SPONSOR/MONITOR'S REPORT NUMBER(S) AFRL-AFOSR-UK-TR-2011-0016	
12. DISTRIBUTION/AVAILABILITY STATEMENT Approved for public release; distribution is unlimited.					
13. SUPPLEMENTARY NOTES					
14. ABSTRACT The goal of the project was to establish the interrelation between the phase interface condition, lattice mismatch of their crystal lattices, crystallographic orientation of the matrix phase relative to the direction of crystallization, thermal expansion coefficient mismatch between constituent phases of the composite, and structure formation processes together with the stress condition in directionally crystallized eutectic composites based on refractory boride compounds. It has been shown that co-orientation of crystal phases is independent from matrix orientation for LaB6-ZrB2 system. Ultrasonic and mechanical investigations have shown the influence of matrix orientation on composite modulus of elasticity. It has been shown that tensile strength of LaB6-ZrB2 DSE at 2000oC exceeds 200 MPa. It has been confirmed that the structural perfection is strongly influenced by the crystallographic orientation of the matrix. An abnormally low heat conductivity was measured for samarium hexaboride at temperatures higher than 1000 C. The influence of thermal coefficient mismatch on internal stress inside the matrix phase in SmB6 - (Ti,Zr)B2 system with varying Ti/Zr is comparable with precision of measurement. These findings can be extended to the related classes of eutectics, and the developed materials can serve as model objects for fundamental research in materials science.					
15. SUBJECT TERMS EOARD, Materials, Ceramics Refractories and Glass					
16. SECURITY CLASSIFICATION OF:			17. LIMITATION OF ABSTRACT SAR	18. NUMBER OF PAGES 32	19a. NAME OF RESPONSIBLE PERSON Stephanie Masoni, Maj, USAF
a. REPORT UNCLAS	b. ABSTRACT UNCLAS	c. THIS PAGE UNCLAS			19b. TELEPHONE NUMBER <i>(Include area code)</i> +44 (0)1895 616420

**THE NATURE OF THE MICROSTRUCTURE AND INTERFACE
BOUNDARY FORMATION IN DIRECTIONALLY SOLIDIFIED
CERAMIC BORIDE COMPOSITES**

Project manager: Filipov Volodymyr Borysovyh

Phone: (+380.44) 424-13-67, Fax: (+380.44) 424-21-31,

E-mail: dep60@ipms.kiev.ua

*Institutions: Frantsevich Institute for Problems of Materials Science
of National Academy of Sciences of Ukraine*

*Financing parties: European Office of Aerospace Research and Development,
United Kingdom*

Operative commencement date:

Project duration: 3 years

Project technical area: Material Sciences

Reported : 01.05.2007 – 31.07.2010

Date of submission: 23.05.2011>

LIST OF FIGURES.....	3
LIST OF TABLES	4
SUMMARY	5
INTRODUCTION.....	5
METHODS, ASSUMPTIONS AND PROCEDURES	6
RESULTS AND DISCUSSION	6
1. Self-reinforced composites with individual diborides as reinforcing phase	6
2. Self-reinforced composites with titanium and zirconium diboride based solid solutions as reinforcing phases	12
2.1. Composite materials $\text{LaB}_6\text{-(Ti}_x\text{Zr}_{1-x})\text{B}_2$	12
2.1.1. Specific features of individual metallic Ti and Zr and their diborides mutual interaction	13
2.1.2. Specific features of mutual interaction in $\text{TiB}_2\text{-ZrB}_2$ system.....	15
2.1.3. Fabrication and testing of single-crystal matrix component inoculants with a certain orientation for further composite growth.....	17
2.1.4. Identification of the eutectic composition in $\text{LaB}_6 - (\text{Ti}_x\text{Zr}_{1-x})\text{B}_2$ system versus x	19
2.1.5. Influence of the composite materials composition on the peculiarities of phase interface formation	21
2.1.6. Main mechanical properties of $\text{LaB}_6\text{-(Ti}_x\text{Zr}_{1-x})\text{B}_2$ composites	22
2.2. Eutectic composition determination in $\text{SmB}_6 - (\text{Ti}_x\text{Zr}_{1-x})\text{B}_2$ system subject to x.....	24
CONCLUSIONS	27
BIBLIOGRAPHY	28
REFERENCES.....	29

- Fig.1. – Microstructure of a $\text{LaB}_6\text{-ZrB}_2$ directionally solidified eutectic composite.
- Fig. 2. – Typical fracture surfaces of a $\text{LaB}_6\text{-ZrB}_2$ composite
- Fig. 3. – Microstructure of a transverse cross-section (a) and longitudinal cross-section (b) of a $\text{LaB}_6\text{-ZrB}_2$ directionally solidified eutectic composite after indentation
- Fig. 4. – Typical microstructure (I) and fracture surfaces micrographs (II) of $\text{LaB}_6\text{-ZrB}_2$ after fracture toughness tests; a-pre-eutectic, b-eutectic, c- past-eutectic compositions, d-composition with addition of 0.2 wt % YB_6 .
- Fig. 5. – Microstructure (SEM): transverse cross-section (a-c) and longitudinal cross-section (d-f), and secondary X-ray specters (g-i) of the directionally solidified $\text{LaB}_6\text{-ZrB}_2$ alloys with varying reinforcing phase content; (a, d, g) – pre-eutectic composition, (b, e, h) –eutectic composition, (c, f, i) – post-eutectic composition.
- Fig. 6. – Microstructure of directionally crystallized lanthanum hexaboride based composites with diborides of transition metals of the IV group of the Periodic System.
- Fig. 7. – SEM images of the longitudinal cross-section of $\text{LaB}_6\text{-ZrB}_2$ samples with excessive LaB_6 (a) (31 mol % ZrB_2) and ZrB_2 (b) (32,5 mol % ZrB_2), respectively.
- Fig.8. – SEM images of transverse cross-section of the $\text{LaB}_6\text{-(Ti}_{0,5}\text{Zr}_{0,5})\text{B}_2$ samples with the excess of LaB_6 (a) (66 mol % LaB_6) and MeB_2 (b) (63 mol % LaB_6), respectively.
- Fig. 9. – Density of Ti-Zr alloys versus composition, ■ - experimental, --- calculated
- Fig. 10. – Young's modulus of Ti-Zr solid solutions versus composition
- Fig. 11. – Concentration dependences of lattice parameters, ("a" and "c"), specific resistance (ρ), microhardness (H) and melting points (T) for $(\text{Ti}, \text{Zr})\text{B}_2$ solid solutions [16].
- Fig. 12. – Deviation of the measured values of «a» and «c» lattice parameters of $\text{TiB}_2\text{-ZrB}_2$ solid solutions from the values calculated according to the additivity law
- Fig. 13. – The setup for inoculant fixation with its orientation necessary for directional crystallization of single crystals.
- Fig.14. – Typical Laue patterns taken from LaB_6 , single crystals used as inoculants.
- Fig.15. – Microstructure of $\text{LaB}_6\text{-(Ti}_x\text{Zr}_{1-x})\text{B}_2$: multi-component samples:
- Fig. 16. – Diboride phase volume in $\text{LaB}_6\text{-(Ti}_{1-x}\text{Zr}_x)\text{B}_2$ eutectic composites versus at % Zr in $(\text{Ti}, \text{Zr})\text{B}_2$
- Fig. 17. – TEM image of $\text{LaB}_6\text{-(Ti}_x\text{Zr}_{1-x})\text{B}_2$ microstructure.
- Fig. 18. – Concentrational dependence of Young's modulus in $\text{LaB}_6\text{-(Ti}_x\text{Zr}_{1-x})\text{B}_2$ composites.
- Fig. 19. – SEM image of the fracture surface after bending tests of $\text{LaB}_6\text{-(Ti}_{0,6}\text{Zr}_{0,4})\text{B}_2$ composition
- Fig. 20. – SEM image of the fracture surface after fracture toughness tests of $\text{LaB}_6\text{-(Ti}_{0,6}\text{Zr}_{0,4})\text{B}_2$ composition
- Fig.21. – Microstructure of a $\text{SmB}_6\text{-(Ti}_x\text{Zr}_{1-x})\text{B}_2$ directionally solidified eutectic composite, a- $x=0$, b- $x=0,20$, c- $x=0,50$, d- $x=0,95$
- Fig.22. – Microstructure of a $\text{SmB}_6\text{-(Ti}_x\text{Zr}_{1-x})\text{B}_2$ directionally solidified eutectic composite, a- $x=0$, b- $x=0,20$, c- $x=0,40$, d- $x=0,80$

LIST OF TABLES

Table 1. – Mechanical properties of alloys in the $\text{LaB}_6\text{-MeB}_2$ system.

Table 2. – Lattice parameters of metallic Ti and Zr [14] and of Ti-Zr solid solutions

Table 3. – Lattice parameters of titanium and zirconium diborides and of their mutual solidsolutions

Table 4. – Initial powder characteristics and sample compositions in the $\text{LaB}_6 - (\text{Ti}_x\text{Zr}_{1-x})\text{B}_2$ system

Table 5. – $\text{LaB}_6 - (\text{Ti+Zr})\text{B}_2$ sample composition produced with diborides synthesized from metals solid solutions

Table 6. – Composition of $\text{LaB}_6 - (\text{Ti+Zr})\text{B}_2$ samples produced from individual diborides

The goal of the project was to establish the interrelation between the phase interface condition, lattice mismatch of their crystal lattices, crystallographic orientation of the matrix phase relative to the direction of crystallization, thermal expansion coefficient mismatch between constituent phases of the composite, and structure formation processes together with the stress condition in directionally crystallized eutectic composites based on refractory boride compounds.

It has been shown that co-orientation of crystal phases is independent from matrix orientation for $\text{LaB}_6\text{-ZrB}_2$ system. Ultrasonic and mechanical investigations have shown the influence of matrix orientation on composite modulus of elasticity. It has been shown that tensile strength of $\text{LaB}_6\text{-ZrB}_2$ DSE at 2000°C exceeds 200 MPa.

Computer simulation accomplished in project P 273 were found to be in good agreement with our experimental results for low crystallization rates ($0,5 \text{ mm/min} < v < 4 \text{ mm/min}$) which enabled to predict the increase of MeB_2 fiber diameter as a function of increasing crystallization rate.

It has been established that the homogeneity of fiber distribution in the matrix phase and the uniformity of the fiber diameter are maximal when the Ti/Zr ratio in the diboride equals 3/2 for $\text{LaB}_6\text{-(Ti,Zr)B}_2$ system. It has been confirmed that the structural perfection is strongly influenced by the crystallographic orientation of the matrix. Stability of directional crystallization is minimal when the matrix orientation [001] is parallel to the heat release direction.

The eutectic relation for $\text{SmB}_6\text{-(Ti}_x\text{Zr}_{1-x})\text{B}_2$ system ($x=0; 0,20; 0,40; 0,60; 0,80; 0,95$) has been determined. For $\text{SmB}_6\text{-(Ti,Zr)B}_2$ system it has been discovered that the excess of titanium atoms in the diboride solid solution results in platelet-like morphology formation for the reinforcing phase.

An abnormally low heat conductivity was measured for samarium hexaboride at temperatures higher than 1000°C . The influence of thermal coefficient mismatch on internal stress inside the matrix phase in $\text{SmB}_6\text{-(Ti,Zr)B}_2$ system with varying Ti/Zr is comparable with precision of measurement. These findings can be extended to the related classes of eutectics, and the developed materials can serve as model objects for fundamental research in materials science.

INTRODUCTION

In recent years, ceramic directionally solidified eutectics (DSEs) have attracted considerable attention because of their thermodynamic compatibility and microstructural stability up to the eutectic invariant point [1]. Oxide DSEs have received the most recent attention because they have demonstrated excellent strength and creep resistance up to high temperatures ($>1200^\circ\text{C}$), which makes them attractive as high-temperature structural materials [2-4]. One limiting property of this class of materials, however, may be the low fracture toughness because the interfaces between the two phases typically adopt low-energy orientation relationships during the directional solidification process, which prevents significant interface de-bonding [5]. On the other hand, while boride DSEs have received relatively less attention, there are indications that these materials may have some advantageous mechanical properties in comparison to their oxide counterparts.

In general, borides of rare-earth and d-transitional metals have outstanding refractory properties with high hardness, high chemical stability and ultra-high melting points that usually range between $2300\text{-}3200^\circ\text{C}$. $\text{LaB}_6\text{-ZrB}_2$ DSEs, which have a eutectic temperature of 2470°C , exhibit high bend strength ($1000\text{-}1320 \text{ MPa}$ [6]) and excellent thermal shock resistance (500 K/min) [7]. Fracture toughness has been investigated in $\text{LaB}_6\text{-ZrB}_2$ DSEs using conventional, macroscopic 3-point bend and Vickers micro-indentation methods. In the conventional tests, $\text{LaB}_6\text{-ZrB}_2$ DSEs showed exceptionally high fracture toughness ($16.3\text{-}27.8 \text{ MPam}^{1/2}$ [6] or $17.8 \text{ MPam}^{1/2}$ [7]) when the initial notches were cut perpendicular to the rod axis. The Vickers indentation method was also utilized by Chen et al. [7], who performed tests on planes parallel and perpendicular to the rod axis, and quantified the fracture toughness as $8.2 \text{ MPam}^{1/2}$ and $8.7 \text{ MPam}^{1/2}$, respectively.

This project aims to thoroughly characterize the microstructure, crystallography and interface structure of $\text{RB}_6\text{-MeB}_2$ (where R – Sm, La, Eu and Me – Ti, Zr, Hf or their solid solution) DSEs and to establish the interrelation between the phase interface condition, lattice mismatch of their crystal lattices, crystallographic orientation of the matrix phase relative to the direction of

crystallization, thermal expansion coefficient mismatch between constituent phases of the composite, and structure formation processes together with the stress condition in directionally crystallized eutectic composites based on refractory boride compounds.

METHODS, ASSUMPTIONS AND PROCEDURES

Composite materials based on lanthanum hexaboride and samarium hexaboride (MeB_6) with both individual titanium or zirconium diborides ($\text{Me}^{\text{II}}\text{B}_2$) and their solid solutions ($\text{Ti}_x\text{Zr}_{1-x}\text{B}_2$) with varying component ratio as a reinforcing phase were chosen for the realization of the present project.

Directional crystallization of alloys that permits to grow the necessary composites directly from the melt was chosen as the processing method for the project objective realization. Under such conditions two phases are simultaneously grown from the melt with a certain mutual crystallographic orientation, which provides the possibility of *in situ* sample formation.

Synthesis and growth of eutectic composite materials by means of directional crystallization was carried out on the “Crystall-111” setup (modernized by the authors) by means of vertical inductive crucible-free zone melting process.

On the first stage of the present investigation starting materials, hexaborides and diborides, were synthesized from high-purity oxides and boron and metal iodides and boron, respectively. Considering the literature data on the interrelation of crystallization parameters of the chosen class of materials and of their mechanical properties with mutual orientation of the matrix phase and eutectic growth direction a considerable amount of time and effort were spent on lanthanum and samarium hexaborides perfect single crystals growth. The latter were used as inoculants for composite materials crystallization with constant orientation. Still another important task was high-precision eutectic composition determination for each material. In particular, a considerable nonlinearity of the diboride volume content in the eutectic composite material based on samarium hexaboride $\text{SmB}_6\text{-Ti}_x\text{Zr}_{1-x}\text{B}_2$ depending on the Ti/Zr ratio in the system was established.

Rod-like samples (4.5-5mm in diameter) of RE-hexaboride based materials reinforced by individual diborides or solid solutions on their base were prepared by the above described method. After certain tooling in order to obtain highly polished surface, samples were investigated by XRD and metallography, and were also passed to the American counterpart (NASA Glenn Centre, Cleveland, USA) for complex analysis according to the project agreements.

RESULTS AND DISCUSSION

1. Self-reinforced composites with individual diborides as reinforcing phase

Rod-like samples of the eutectic composite material on the base of lanthanum hexaboride (LaB_6) reinforced with zirconium diboride (ZrB_2) fibers were grown by directional crystallization. This material is of primary interest for further investigations as a possible model object for in-depth elucidation of the nature of behavior of composites based on other refractory compounds of related types (oxides, carbides, silicides, etc.).

It has been established that self-reinforced ceramic composites formed on the base of RE and transition metals eutectics [8, 9] have enhanced mechanical properties, especially bending strength and fracture toughness, and therefore these materials can be classified as “tough ceramics”.

XRD phase analysis together with metallography investigations revealed that the composites under investigation have no mutual solubility between their constituent phases, are homogeneous, fine-grained, and their microstructure consists of single-crystal lanthanum hexaboride matrix where diboride single-crystal fibers of largely equal thickness are homogeneously distributed. Such a highly perfect microstructure must guarantee enhanced mechanical properties [8-10] (Fig.1).

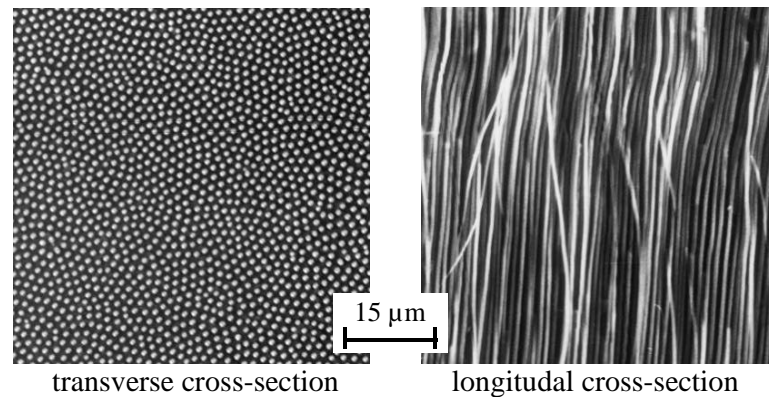


Fig.1. – Microstructure of a $\text{LaB}_6\text{-ZrB}_2$ directionally solidified eutectic composite.

Enhanced mechanical properties, in particular remarkable fracture toughness, of self-reinforced materials of this type are conditioned by their unique microstructure. Crack propagation and failure resistance in such materials are determined by the energy necessary for the fracture surface formation: the higher this energy, the higher is the strength of the material. Fracture surface formed in such material has a complex nature: shear fracture of the matrix phase, fiber pull-out from the matrix, and fracture of the reinforcing fibers themselves are observed simultaneously (Fig.2). Crack propagation in the material is non-linear, as a rule occurring along the fibers, resulting in an “arborescent” fracture surface. (Fig. 2, b).

The main factor causing hindering of crack formation and propagation in such materials and, as a result, of their enhanced strength and fracture toughness is crack deflection on the reinforcing fibers (Fig. 3, a).

Apparently such mechanism of crack propagation occurs due to the absence of any chemical interaction between the matrix phase and the fibers as it has been shown earlier [9, 11], and the respective phase interface is clean, i.e., no intermediate layer (transition layer) is formed between the matrix and the fiber.

It has been established that crack propagation in the matrix phase along the plane perpendicular to the fibers does not result in the immediate disruption of the latter. On the initial stage deformation of the fibers occurs, and only on the next stage disruption is observed at a certain distance from the crack propagation plane. It is logical to assume that the fracture mechanism of the self-reinforced ceramic materials is determined by a combination of factors such as matrix strength, crack propagation in the matrix phase, crack deflection on the matrix-fiber interface, fiber strength, etc. Fracture is accompanied by the fiber pull-out from the matrix and multiple crack deflection along the fibers, which results in a so-called “arborescent” fracture surface formation. Such fracture mechanism requires additional energy for crack propagation [11]. The fiber pull-out as the prevailing fracture mechanism of the RE- and transition metal boride based directionally crystallized eutectic ceramic composites is confirmed by microstructural investigations of their fracture surfaces. As it can be seen from Fig. 2 (a, b) fragments of fibers pulled out from the matrix phase and grooves in the matrix from where the fibers were removed are clearly seen on the fracture surface.

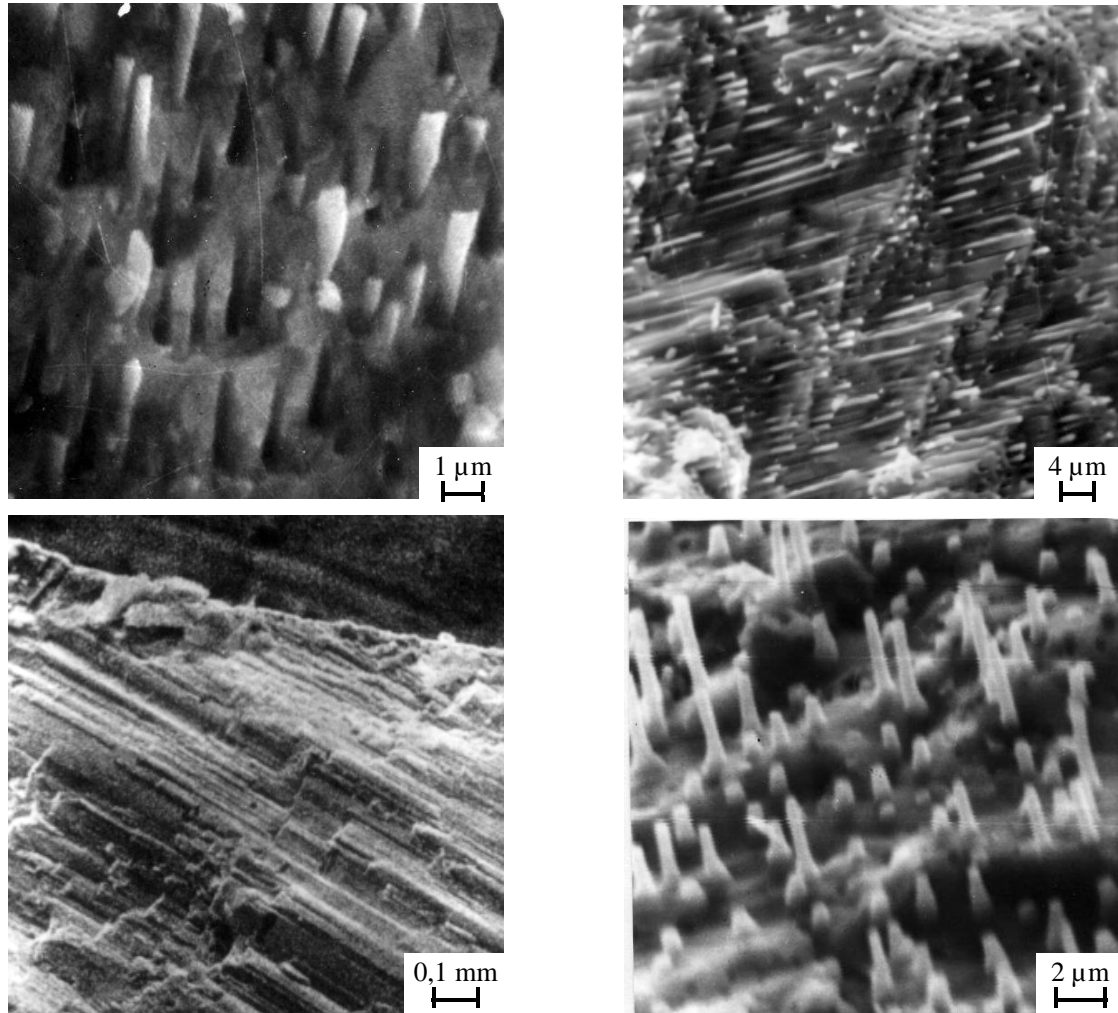


Fig. 2. – Typical fracture surfaces of a $\text{LaB}_6\text{-ZrB}_2$ composite

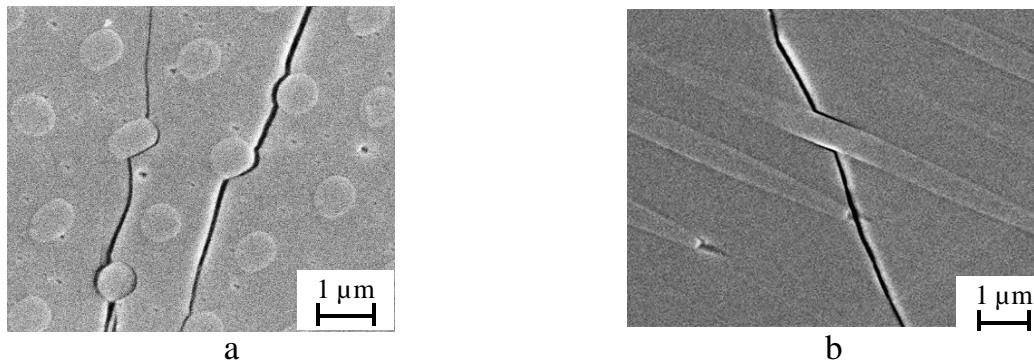


Fig. 3. – Microstructure of a transverse cross-section (a) and longitudinal cross-section (b) of a $\text{LaB}_6\text{-ZrB}_2$ directionally solidified eutectic composite after indentation

Fracture toughness (K_{Ic}) of such composite is therefore determined not only by the strength and the number of the reinforcing fibers but, largely, by the extra work necessary for fiber deformation and their pull-out from the matrix. As it has been shown previously, diboride fibers are single-crystalline and have a perfect real structure [6, 11].

Severe crack deflection by the reinforcing fibers occurs during crack propagation in the matrix phase. Moreover, the matrix prevents the possibility of fiber bending or twisting therefore the fibers are subjected to uniaxial tension. Simultaneously, they are subjected to a relatively severe radial compression from the matrix due to the thermal expansion coefficient mismatch of the matrix and the fibers, the degree of compression being determined by the value of the said mismatch.

Therefore, considering the single crystal nature of the fibers their strength is likely to be sufficiently higher than that of a bulk material of the same composition. Specifics of the stress condition that governs fiber fracture mechanism is confirmed by certain indications of their plastic deformation preceding fracture: formation of a neck during fiber rupture even if the fracture toughness tests are conducted at room temperature (Fig. 2, c).

It should be specifically noted that due to numerous crack deflections along the fiber growth direction its propagation normally occurs at an angle (up to 70^0) to the load application direction (Fig. 4).

composition is additionally confirmed by extreme sensibility of mechanical properties to the homogeneity of their structure and, hence, to the deviations from the eutectic composition itself.

Excess of either matrix or reinforcing phase in the composite material produced by directional crystallization from individual borides results in a periodic crystallization of the extra phases.

It has been established that the regularity of investigated composite materials structure considerably depends on the deviation of the system from the eutectic composition: deviation in either of possible directions results in structure changes and dramatic deterioration of their mechanical properties (see Table 1).

Table 1. – Mechanical properties of alloys in the $\text{LaB}_6\text{-MeB}_2$ system.

Material	Bending strength, σ , MPa	Fracture toughness K_{Ic} , MPa. m ^{1/2}
LaB_6 , fracture along the(100) plane	200...234	3,0...3,4
$\text{LaB}_6\text{-ZrB}_2$ (eutectic)	1000...1320	15,2...18,3
$\text{LaB}_6\text{-TiB}_2$ (eutectic)	1150...1250	11,0...14,4
$\text{LaB}_6\text{-HfB}_2$ (eutectic)	388...656	15,2...16,5
$\text{LaB}_6\text{-TiB}_2$ (pre- eutectic composition)	-	5,0...6,0
$\text{LaB}_6\text{-TiB}_2$ (post- eutectic composition)	-	9,2...10,0
$\text{LaB}_6\text{-TiB}_2\text{-ZrB}_2$ (pre- eutectic composition)	-	5,2-6,7
$\text{LaB}_6\text{-ZrB}_2\text{-HfB}_2$ (pre- eutectic composition)	-	4,7...6,0
$\text{LaB}_6\text{-TiB}_2\text{-HfB}_2$ (pre- eutectic composition)	-	5,5...7,2
$\text{LaB}_6\text{-TiB}_2\text{-ZrB}_2\text{-HfB}_2$ (pre- eutectic composition)	-	4,7...6,0
$\text{LaB}_6\text{-TiB}_2\text{-ZrB}_2\text{-HfB}_2$ (eutectic)		10,4...17,5
$\text{LaB}_6\text{-ZrB}_2$ (eutectic)+ 0,2 wt % YB_6	~ 1200	5,2...9,0

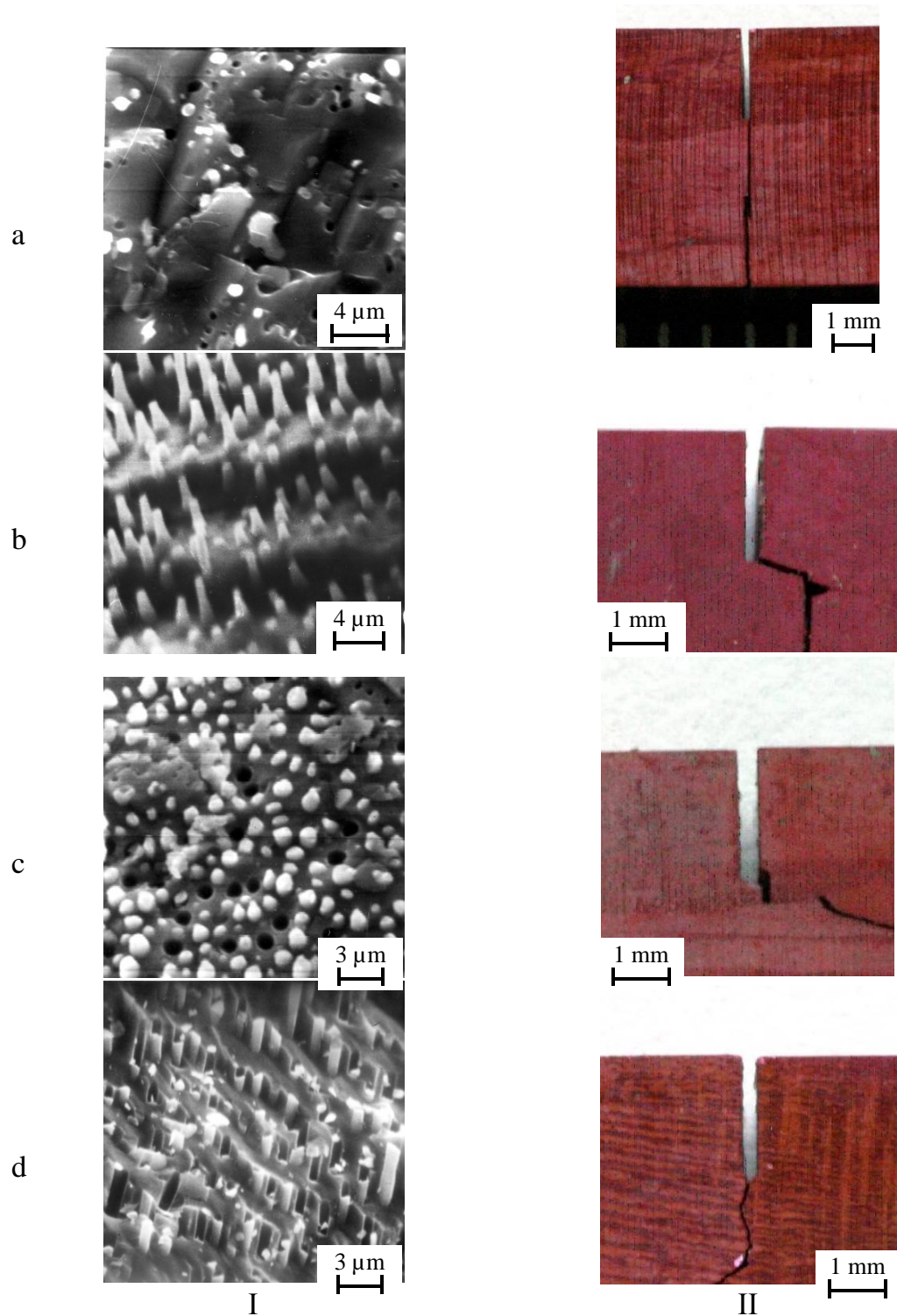


Fig. 4. – Typical microstructure (I) and fracture surfaces micrographs (II) of LaB₆-ZrB₂ after fracture toughness tests; a-pre-eutectic, b-eutectic, c- past-eutectic compositions, d- composition with addition of 0.2 wt % YB₆.

The fact that the above described fracture mechanism is typical for the materials of eutectic It has been shown that the excess of either matrix or reinforcing phase in a directionally solidified composite material results in a periodic crystallization of the excess of such a phase and to decoration of the crystallization front (Fig. 5).

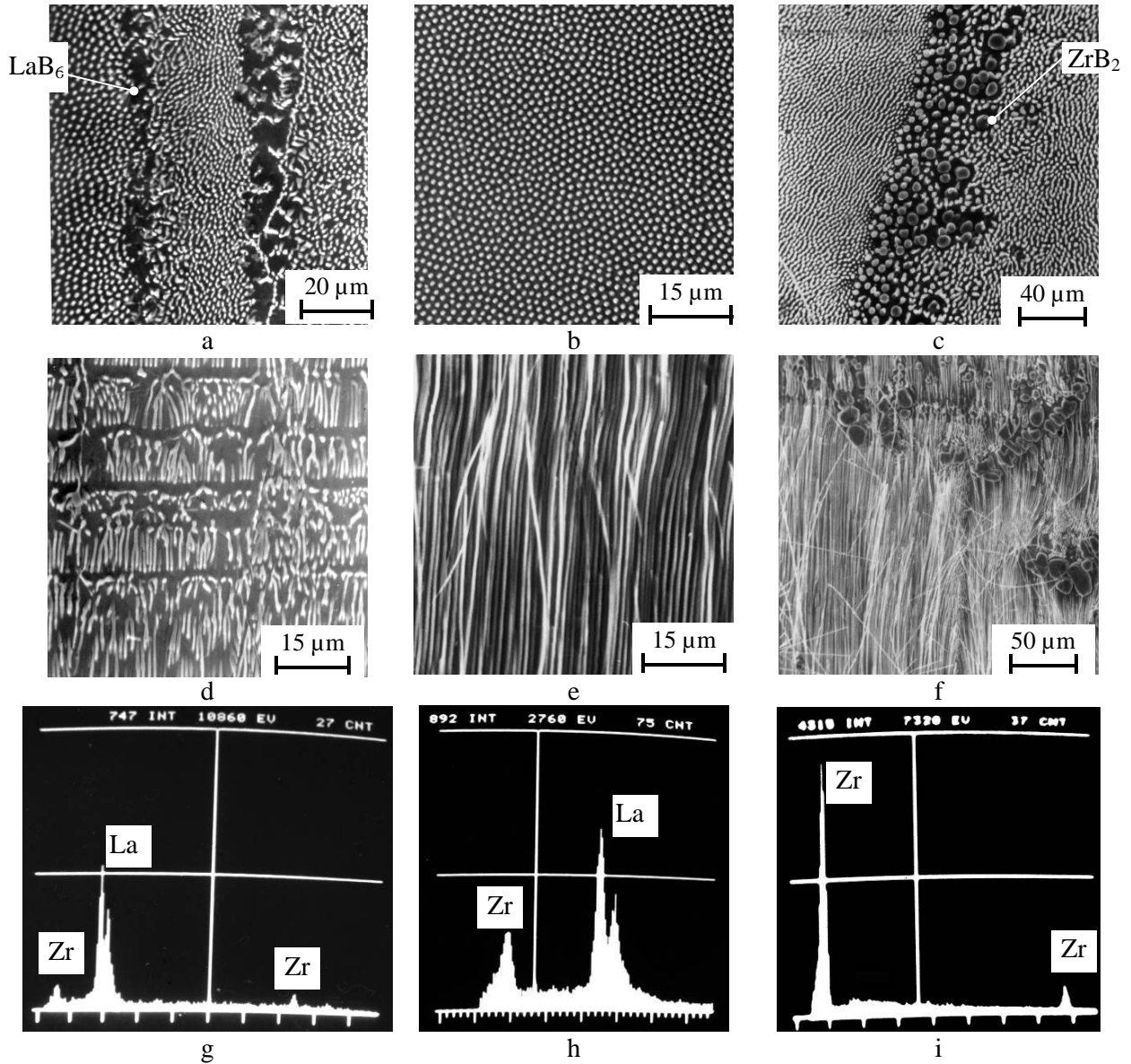


Fig. 5. – Microstructure (SEM): transverse cross-section (a-c) and longitudinal cross-section (d-f), and secondary X-ray spectra (g-i) of the directionally solidified $\text{LaB}_6\text{-ZrB}_2$ alloys with varying reinforcing phase content; (a, d, g) – pre-eutectic composition, (b, e, h) – eutectic composition, (c, f, i) – post-eutectic composition.

Excessive amounts of matrix phase (LaB_6) crystallize as continuous interlayers (Fig.5, a, d). Along these interlayers failure of the material occurs and the fracture toughness decreases dramatically down to $5\text{--}6 \text{ MPa m}^{1/2}$, i.e. to the K_{Ic} level of the pure lantahanum hexaboride. The excessive amounts of the reinforcing phase (ZrB_2) do not form continuous layers and appear in the form of large spherical inclusions thus disrupting the uniformity of the fibers both in longitude and diameter (Fig.5, c, f). This also results in the failure of the material along such inclusions, which also results in the K_{Ic} decrease, however not as dramatic one as in the first case (Table 1).

These findings can be applied to the related classes of eutectics and the materials under investigation can be used as the model objects for fundamental materials science research.

2. Self-reinforced composites with titanium and zirconium diboride based solid solutions as reinforcing phases

2.1. Composite materials $\text{LaB}_6-(\text{Ti}_x\text{Zr}_{1-x})\text{B}_2$

In our early works [12] it has been shown that a uniform fiber structure is also observed in directionally crystallized lanthanum hexaboride based composites with the reinforcing phase formed from the solid solutions of diborides of transition metals of the IV group of the Periodic System (Fig. 6).

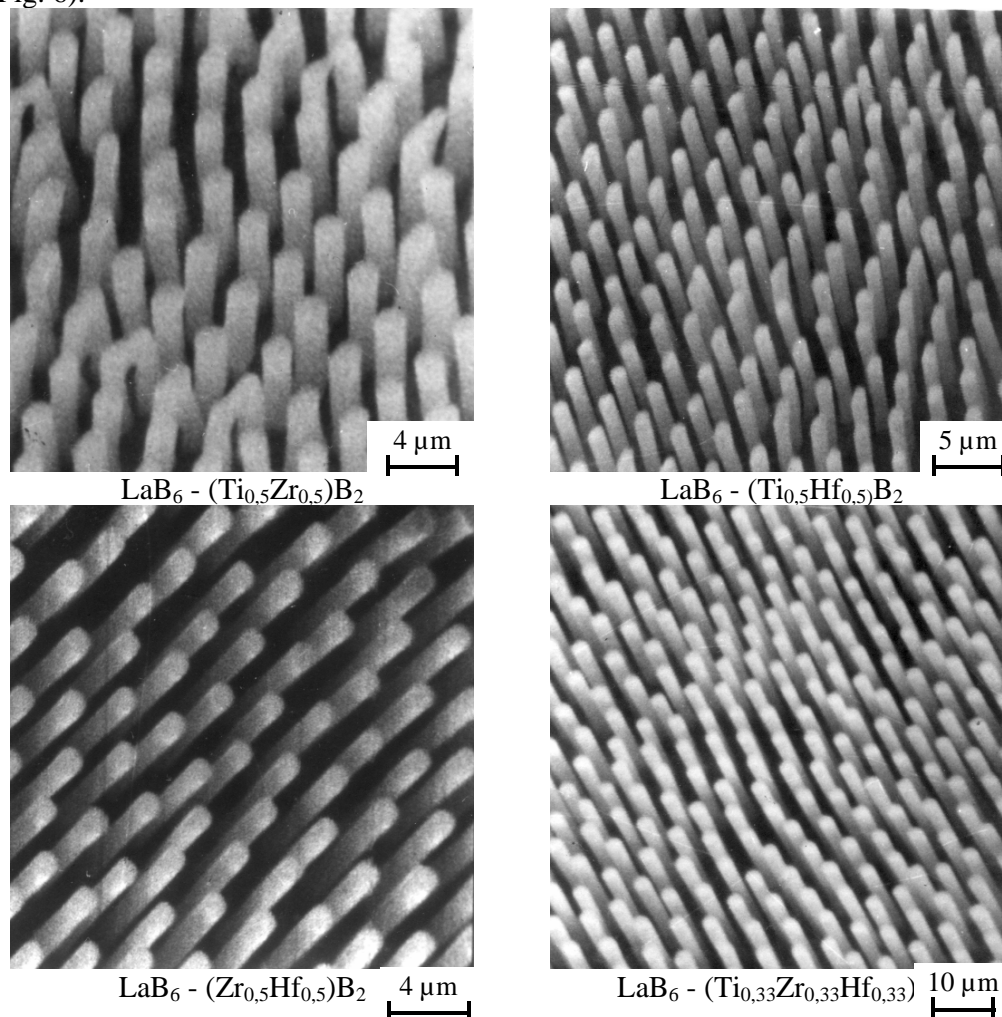


Fig. 6. – Microstructure of directionally crystallized lanthanum hexaboride based composites with diborides of transition metals of the IV group of the Periodic System.

If the fibers (whiskers) are formed from the diboride solid solutions the degree of structure perfection and, hence, the mechanical properties of the composite are less sensitive to minor compositional changes compared to the use of pure diborides which is related with the broadening of the eutectic region of existence in multicomponent systems [13].

In eutectic alloys in $\text{LaB}_6-(\text{Ti}_{1-x}\text{Zr}_x)\text{B}_2$ system the interatomic B-B distance in the plain boron lattice of the diboride phase and/or of the boron octahedron of lanthanum hexaboride at room temperature increases in the following order: $\text{TiB}_2 \rightarrow \text{LaB}_6 \rightarrow \text{ZrB}_2$. Considering the known literary data for the thermal expansion coefficients of these materials it can be assumed that this pattern is also true for the temperatures of eutectic crystallization. If the above mentioned interatomic distances match the boron sublattices of the two phases will be better conjugated and the process of their co-crystallization will be facilitated. This will influence the proportion of these phases in the forming eutectic resulting in enhanced structure homogeneity and, therefore, structure-sensitive mechanical properties.

If individual diborides are used as reinforcing components mechanical properties of the directionally solidified composites become rather sensitive to the slightest deviations from the eutectic composition due to the structure homogeneity (regularity) breach resulting from excessive phase interlayers formation on the crystallization front (Fig. 7) [6].

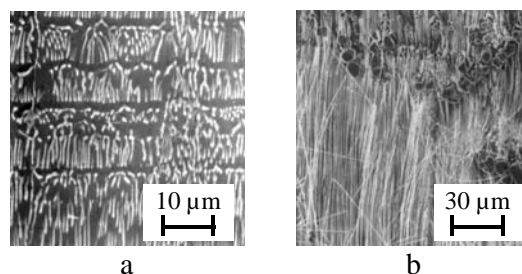


Fig. 7. – SEM images of the longitudinal cross-section of LaB_6 - ZrB_2 samples with excessive LaB_6 (a) (31 mol % ZrB_2) and ZrB_2 (b) (32,5 mol % ZrB_2), respectively.

It becomes possible to radically change the structure formation conditions if the diboride solid solutions are used instead of pure diborides. In such case the excessive phase tends to crystallize in the form of equilibrium crystals (Fig.8) [12], and the sensitivity of mechanical properties of the resulting material to the slight compositional changes becomes less pronounced.

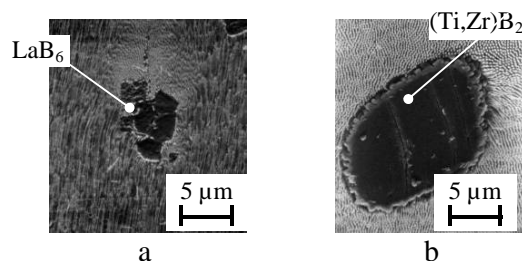


Fig.8. – SEM images of transverse cross-section of the LaB_6 -($\text{Ti}_{0,5}\text{Zr}_{0,5}$) B_2 samples with the excess of LaB_6 (a) (66 mol % LaB_6) and MeB_2 (b) (63 mol % LaB_6), respectively.

In order to achieve the possibility of mechanical properties tailoring of such complex composites it is necessary to understand the fundamental regularities of interaction of both individual metals (Ti and Zr) and of their diborides (TiB_2 and ZrB_2).

As it has been shown earlier, the relation between the volume of diboride phase in eutectic alloys of LaB_6 – ($\text{Ti}_x\text{Zr}_{1-x}$) B_2 system and the Ti/Zr ratio is a nonlinear one. Considering that the amount of impurities in commercial diboride powders is high and unpredictable we studied this relation using high purity starting materials: iodide titanium and zirconium, and high-purity amorphous boron. In order to establish the influence of Ti and Zr distribution homogeneity in diboride solid solution on phase interface formation we have investigated the Ti-Zr solid solution formation process.

2.1.1. Specific features of individual metallic Ti and Zr and their diborides mutual interaction

By means of structural X-ray analysis (HZG-4A) lattice parameters of pure metallic Ti and Zr produced by arc melting were determined. These metals were further used for preparation of diborides. Lattice spacing change of Ti-Zr solid solutions in relation with the component ratio has been calculated using additive law (see Table 2).

As it can be seen from the data presented in Table 2, measured lattice parameters of Ti-Zr solid solutions are in complete agreement with the ones calculated using the additive law.

Table 2. – Lattice parameters of metallic Ti and Zr [14] and of Ti-Zr solid solutions

Lattice parameter, Å	Ti	Ti-Zr alloys, mol%				Zr
		20/80	40/60	60/40	80/20	
<i>a</i>	2.9505	3,1757	3,1194	3,0631	3,0068	3
<i>c</i>	4,6826	5,0541	4,9611	4,8682	4,7752	5,147
<i>c/a</i>	1,5841	1,5915	1,5904	1,5893	1,5881	1,593

Concentration dependence of density and Young's modulus for Ti-Zr solid solutions have been established. The results are presented in Fig. 9 and 10. As it can be observed, the calculated data for density are somewhat higher than the experimental ones, which indicates that the solid solutions formed in this system are most probably of substitutional type (calculations were made according to the method suggested in [15]). The compositional dependence of Young's modulus for Ti-Zr solid solutions is a non-linear one (Fig.10), indicating that bonding rigidity between the dissimilar atoms is somewhat lower than that between the similar ones.

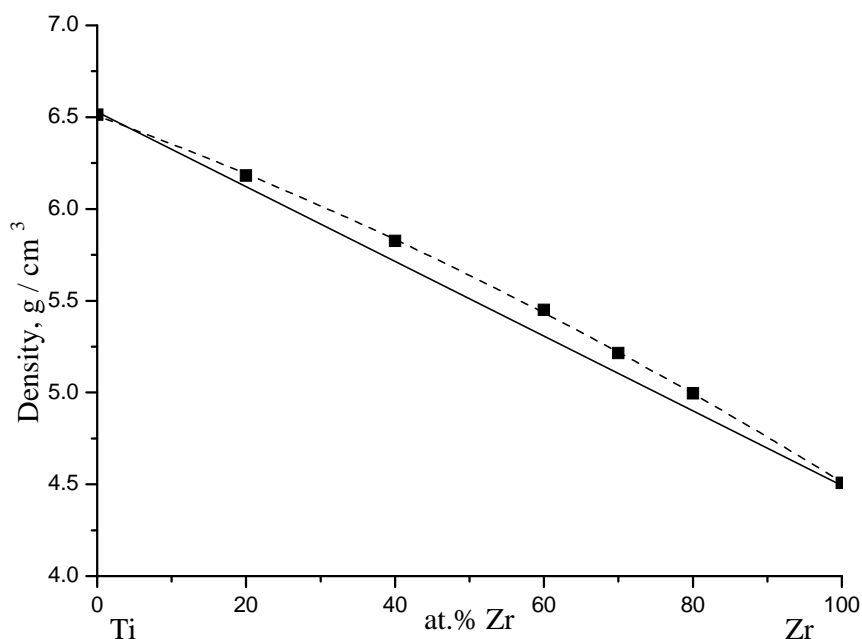


Fig. 9. – Density of Ti-Zr alloys versus composition, ■ - experimental, --- calculated

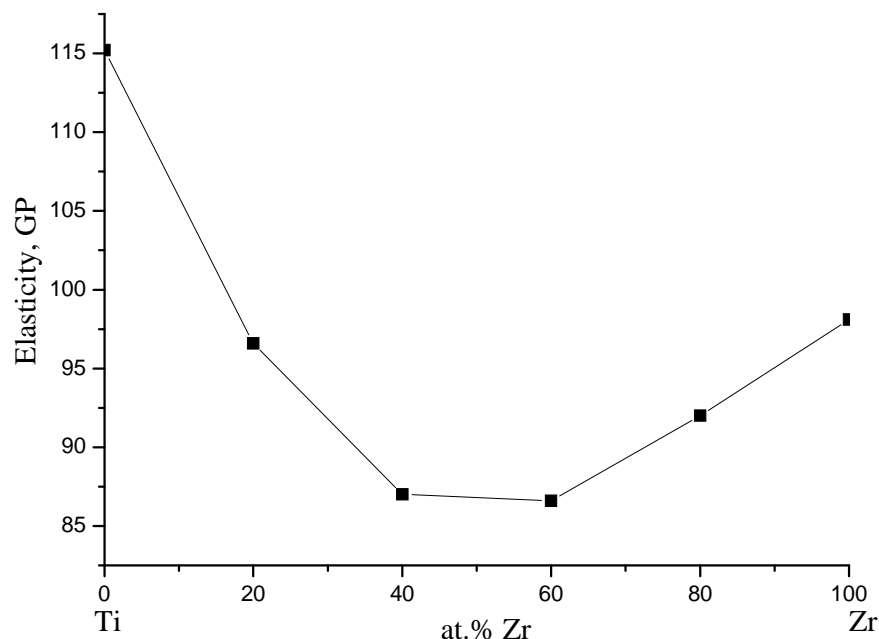


Fig. 10. – Young's modulus of Ti-Zr solid solutions versus composition

2.1.2. Specific features of mutual interaction in $\text{TiB}_2\text{-ZrB}_2$ system

The following isomorphic conditions must be met for a continuous solid solutions formation: similarity of crystal lattices, atomic similarity of components, forming the compound, same type of chemical bonding, presence of the same element in all forming compounds, same stoichiometric composition of the compounds formed and a continuous range of solid solutions formation between the metals forming the interacting compounds [16]. Application of this analysis to the phases of interstitial type has shown that the necessary and sufficient condition of a continuous solid solution range formation for such phases is their isomorphism, same type of chemical bonding, and the continuous range of solid solutions formation by the metals forming the compounds under scrutiny.

A number of works [17-26] confirmed an unlimited mutual solubility of components in the quasibinary $\text{TiB}_2\text{-ZrB}_2$ system. At the same time, a non-monotonic change of a number of concentrational dependences, in particular of specific resistance, microhardness and melting points has been observed for this system (Fig. 11).

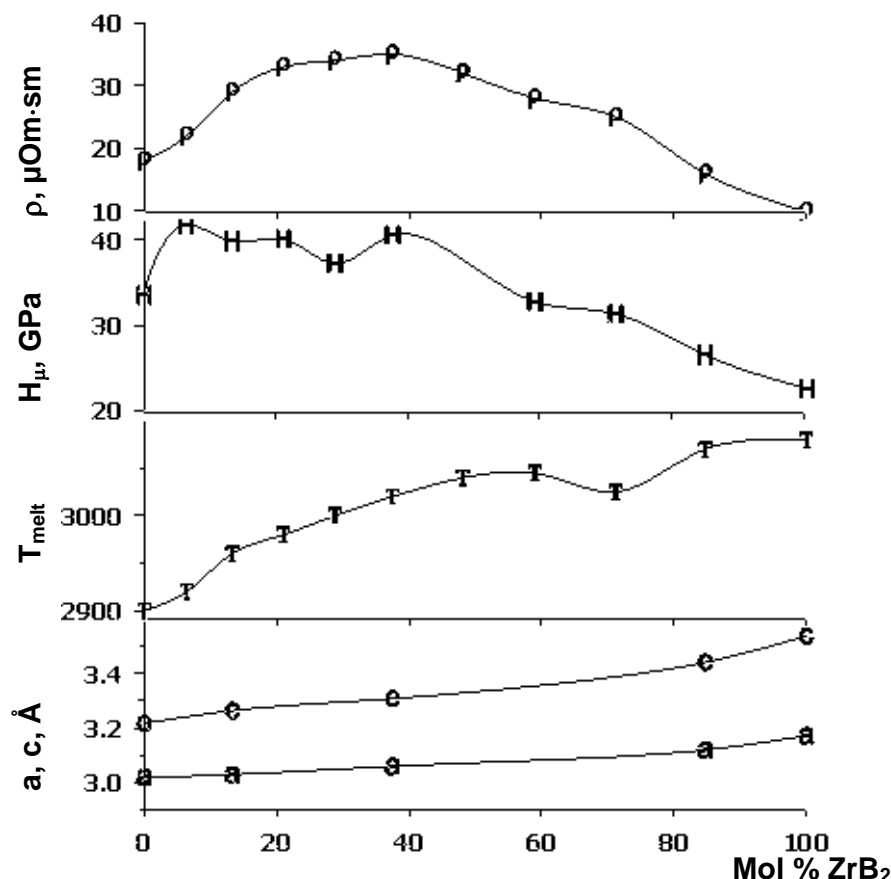


Fig. 11. – Concentration dependences of lattice parameters, (“a” and “c”), specific resistance (ρ), microhardness (H) and melting points (T) for $(\text{Ti}, \text{Zr})\text{B}_2$ solid solutions [16].

Authors of the present research in one of the earlier works [17] came to a conclusion that diffusion in the TiB_2 - ZrB_2 system occurs according to the following mechanism: exclusively metallic atoms are mobile while the boron atoms that are arranged in the so-called boron networks remain static and do not take part in the diffusion processes.

As it was mentioned previously, commercial diboride powders have a relatively high and non-reproducible impurity content. This fact triggered our effort to study the process of TiB_2 and ZrB_2 solid solutions formation using the high-purity starting materials. Therefore, initially only four compositions of titanium-zirconium diboride solid solutions $(\text{Ti}_x\text{Zr}_{1-x})\text{B}_2$ produced by arc melting from $(\text{Ti}_x\text{Zr}_{1-x})$ and crystal boron were studied (Table 2). The use of crystal boron enabled us to somewhat decrease the reaction rate during boride synthesis.

Diborides produced by arc melting for further use in alloy fabrication were investigated by XRD structural analysis using HZG-4A diffractometer. Lattice parameters of titanium and zirconium diborides and of their mutual solid solutions were measured. Calculation of lattice parameters was performed using all XRD reflexes in the range of angles 2θ from 34,6 up to 102,8 degrees and compared with the literary table data (Table.3), (Fig.12).

Table 3. – Lattice parameters of titanium and zirconium diborides and of their mutual solidsolutions

Lattice parameter	Method of determination	Titanium diboride	Ti/Zr ration in the solid solution, at %				Zirconium diboride
			20/80	40/60	60/40	80/20	
<i>a</i>	calculated	3,028	3,141	3,113	3,084	3,056	3,169*
	experimetal	3,033	3,151	3,118	3,089	3,063	3,171
<i>c</i>	calculated	3,228	3,470	3,409	3,349	3,288	3,530*
	experimental	3,231	3,497	3,427	3,373	3,301	3,533

* literary data

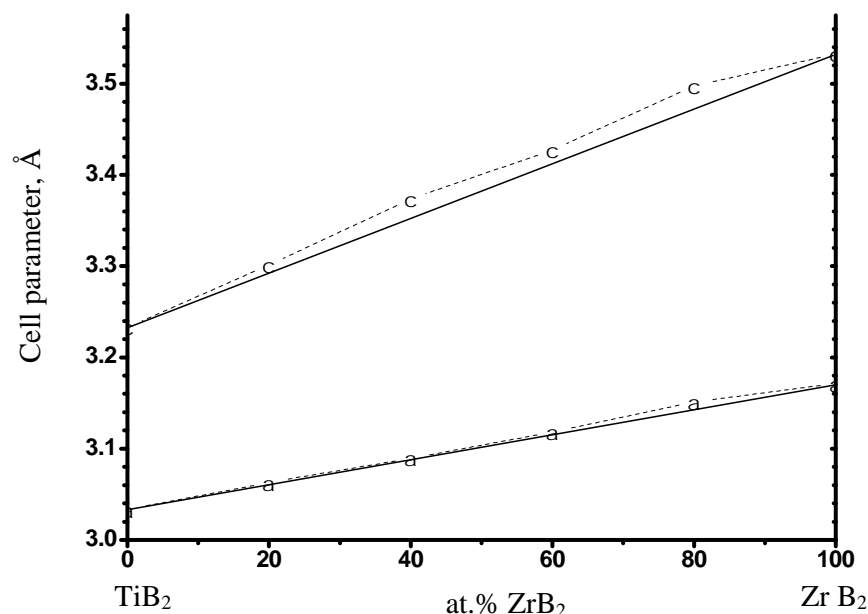


Fig. 12. – Deviation of the measured values of «a» and «c» lattice parameters of TiB₂–ZrB₂ solid solutions from the values calculated according to the additivity law

As it can be seen from the presented results, a slight difference between the calculated and experimental data is observed. Both «a» and «c» experimental lattice parameters deviate to higher values than the calculated ones, though the deviation of «c» is somewhat higher than the one of «a».

2.1.3. Fabrication and testing of single-crystal matrix component inoculants with a certain orientation for further composite growth

Latest data present convincing evidence that the highest properties of the materials produced by zone melting are achieved on the single crystals of highest purity and perfection that also have the most effective crystallographic orientation. For example, in the case of emitters from lanthanum hexaboride an anisotropy of thermal electron emission work function is observed depending on the crystallographic orientation of the single crystal plane. The use of emitters with specific orientation must result in the decrease of the cathode working temperature by 200-300K without any decrease in emission output. This is of immense importance for cathode unit construction optimization, extension of the cathode unit lifetime, of the cathode lifetime, and of the energy consumption for heating and emission.

LaB₆ single crystals are characterized by a pronounced mechanical properties anisotropy [27] due to the cleavage plane (001) existence in its crystal structure, which is typical for all materials with the CaB₆ structure type. This results in exceptionally easy crack propagation along this plane and even in the possibility of ready chipping of thin platelets from the LaB₆ single crystals along this plane. It seems highly plausible that the same effect of properties anisotropy must be present in metal diborides including anisotropy of thermal expansion coefficient. Considering this assumption and the formation of a state of stress inside the composite upon cooling due to the thermal expansion coefficient mismatch between the matrix and the fibers, and the said anisotropy of the diboride phase an in-depth study of the influence of the matrix phase orientation on composite mechanical properties has been accomplished.

Moreover, properties investigation of the directionally crystallized eutectic composites suggests that phase interface conditions between eutectic colonies must have a determinative influence because they disrupt the materials homogeneity. Since LaB₆ is the nucleating phase in LaB₆ - MeB₂ composites an assumption has been made that the use of a single crystal LaB₆

inoculant must enhance the growth of the rods with the majority of their cross-section consisting of a single eutectic colony.

For LaB_6 single crystal growth with the necessary crystallographic orientation a special grip was used that enabled to mount the samples at an angle of 40° to the crystal growth direction (Fig.13). Thus grown crystals were checked for the crystallographic orientation and, if necessary, the process was repeated. Microstructure of the grown crystals was performed by metallographic methods (the presence of the grain boundaries was determined) and by X-ray methods (Laue patterns were taken). Samples for these investigations were prepared according to the metallographic procedure described in detail in the Chapter 4 of the present report. After multiple-stage polishing the surface of the samples was etched by the (1:1) aqueous solution of the nitric acid at room temperature for 30s. Laue patterns revealed the deviation angle of the necessary crystallographic direction from the axis of the grown crystal as well as its degree of perfection in the area of 1.2 mm in diameter. (Fig.14).



Fig. 13 – The setup for inoculant fixation with its orientation necessary for directional crystallization of single crystals.

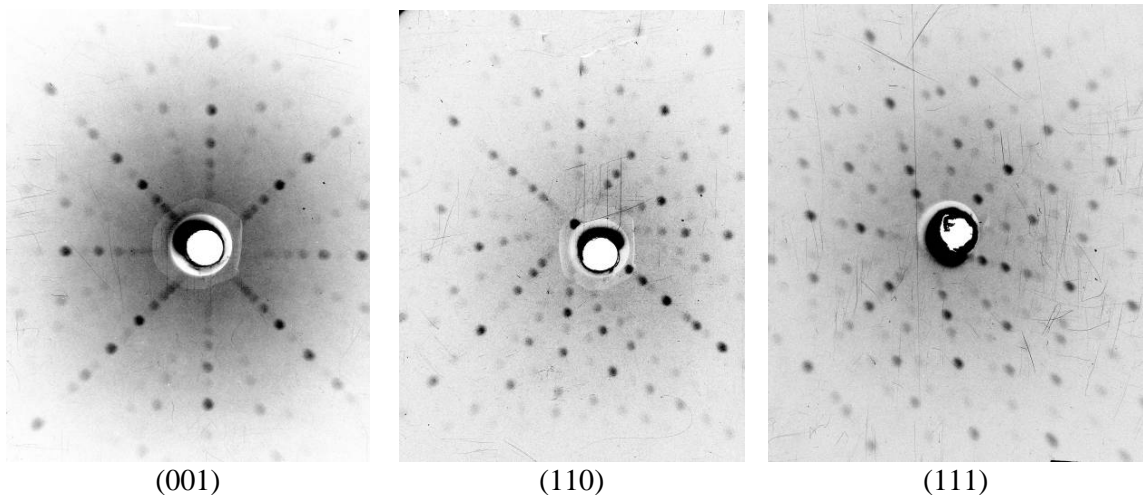


Fig.14 – Typical Laue patterns taken from LaB_6 , single crystals used as inoculants.

2.1.4. Identification of the eutectic composition in $\text{LaB}_6 - (\text{Ti}_x\text{Zr}_{1-x})\text{B}_2$ system versus x

Taking into account that the volume content of the diboride phase in its eutectic with LaB_6 for the $\text{LaB}_6 - \text{TiB}_2$, $\text{LaB}_6 - \text{Ti}_{0,5}\text{Zr}_{0,5}\text{B}_2$ and $\text{LaB}_6 - \text{ZrB}_2$ alloys has a nonlinear character we have accomplished a high-precision investigation of the exact eutectic composition on the $\text{LaB}_6 - (\text{Ti}_x\text{Zr}_{1-x})\text{B}_2$ system versus x . The previous stage of research [8] has been accomplished using the commercial individual boride and lanthanum hexaboride powders. Their main characteristics and sample compositions are given in Table 4.

Table 4. – Initial powder characteristics and sample compositions in the $\text{LaB}_6 - (\text{Ti}_x\text{Zr}_{1-x})\text{B}_2$ system

Sample #	I	II	III	IV	V	VI	VII
Ti (at %)	0,95	0,9	0,9	0,8	0,8	0,7	0,6
Zr (at %)	0,05	0,1	0,1	0,2	0,2	0,3	0,4
$\text{Ti}_x\text{Zr}_{1-x}\text{B}_2$ (ob %)	12,0	12,5	13,0	14,5	15,0	16,0	17,0
LaB_6 (ob %)	88,0	87,5	87,0	85,5	85,0	84,0	83,0

Microstructure of the produced samples was studied by optical and electron microscopy.

As it was expected all compositions upon crystallization produced eutectic structure where lanthanum hexaboride forms the matrix phase and a diboride phase forms the reinforcing phase. However, the first experiments were not completely successful in the sense of exact eutectic composition choice, and in all samples a certain excess of diboride phase was present (Fig. 15).

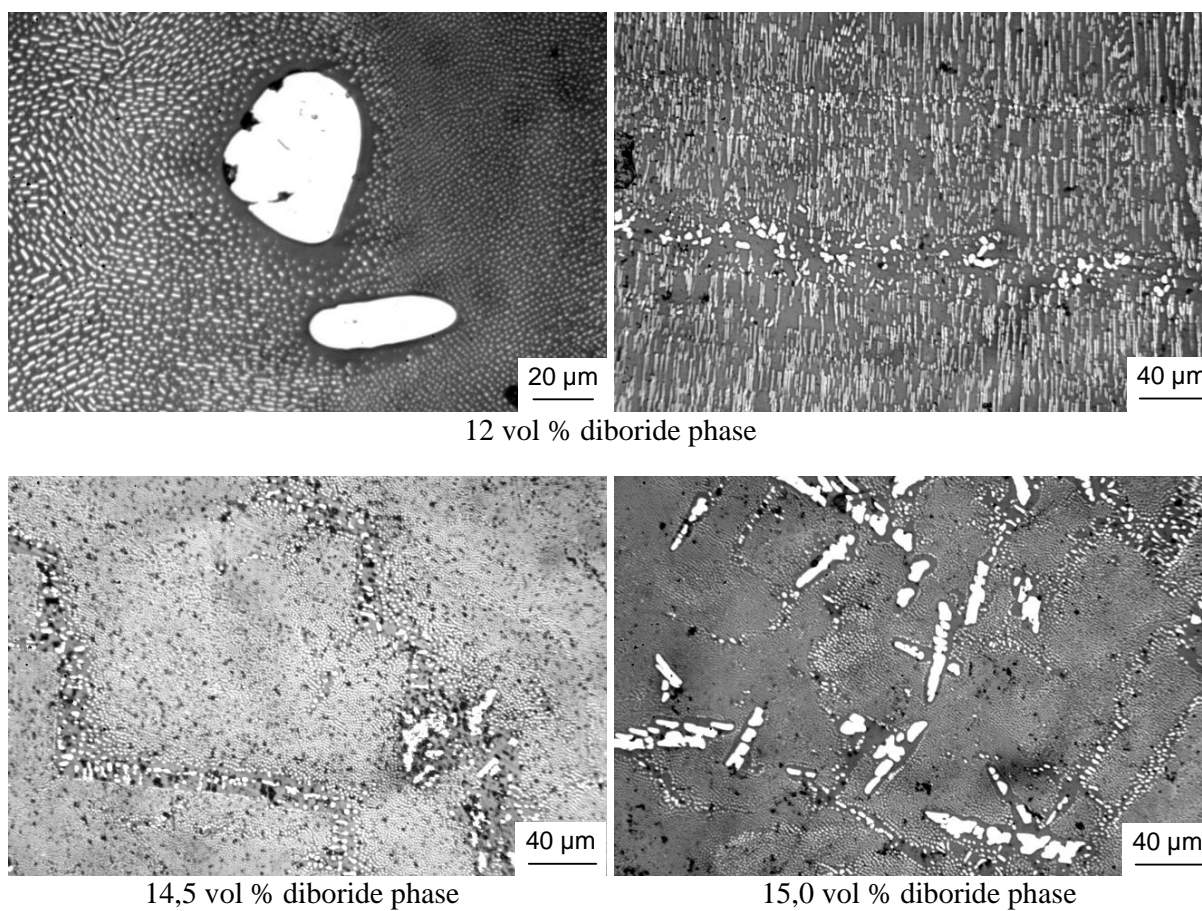


Fig.15 – Microstructure of $\text{LaB}_6 - (\text{Ti}_x\text{Zr}_{1-x})\text{B}_2$: multi-component samples:

As it has been already mentioned, the volume of the diboride phase has a nonlinear dependence from the Ti/Zr ratio in eutectic alloys of the $\text{LaB}_6 - (\text{Ti}_x\text{Zr}_{1-x})\text{B}_2$ system. Taking into account a relatively high and unreproducible amount of impurities in commercial diboride powders this dependence was studied using high-purity powders prepared in our laboratory following the method described previously. LaB_6 powder was produced by the borothermic process (see Table 5 and Fig.16).

Table 5. – $\text{LaB}_6 - (\text{Ti}+\text{Zr})\text{B}_2$ sample composition produced with diborides synthesized from metals solid solutions

Sample number	I-2	II-2	III-2	IV-2
Ti (at %)	80	60	40	20
ZrB (at %)	20	40	60	80
$(\text{Ti}+\text{Zr})\text{B}_2(\text{vol}\%)$	13,0	15,5	17,5	17,5
$\text{LaB}_6(\text{vol}\%)$	87,0	84,5	82,5	82,5

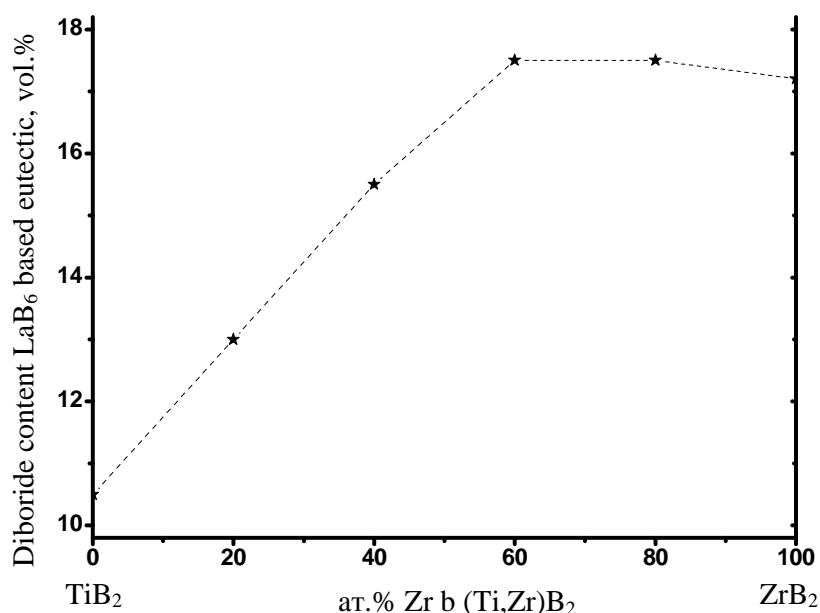


Fig. 16. – Diboride phase volume in $\text{LaB}_6 - (\text{Ti}_{1-x}\text{Zr}_x)\text{B}_2$ eutectic composites versus at % Zr in $(\text{Ti},\text{Zr})\text{B}_2$

In order to elucidate the influence of Ti/Zr ratio on eutectic composition and the importance of diboride solid solutions processing on the properties of the eutectic alloys an in-depth study of a number of alloys with varying Ti/Zr ratio has been accomplished (Table. 6). Solid solution diborides produced by arc melting of individual diborides and individual diborides mixtures in the necessary proportion were used as starting materials. The results of these experiments confirmed our hypothesis that due to a considerable melt volume during zone melting eutectic alloys structure formation does not depend on the initial processing of the diboride solid solution.

Table 6. – Composition of $\text{LaB}_6 - (\text{Ti}+\text{Zr})\text{B}_2$ samples produced from individual diborides

Sample number	1	2	3	4	5	6	7	8
TiB_2 (mol %)	90	80	75	70	60	50	40	20
ZrB_2 (mol %)	10	20	25	30	40	50	60	80

The amount of boron was calculated in such way as to have the desirable $(\text{Ti}_x\text{Zr}_{1-x})\text{B}_2$ diboride solid solution composition.

The accomplished study confirmed the dramatic change of the diboride phase volume in the $\text{LaB}_6 - (\text{Ti}_x\text{Zr}_{1-x})\text{B}_2$ eutectic alloys with the change of Zr (at %) content in the solid solution diboride near the equiatomic composition. Probably, this is related with the peculiarities of interaction on the phase interface during alloy crystallization. For better understanding of the latter we must calculate the relevant lattice parameters at the temperatures equal to the eutectic crystallization ones. In order to fulfill this goal we plan to investigate the thermal expansion coefficients of the constituent phases up to the temperatures close to the eutectics melting points.

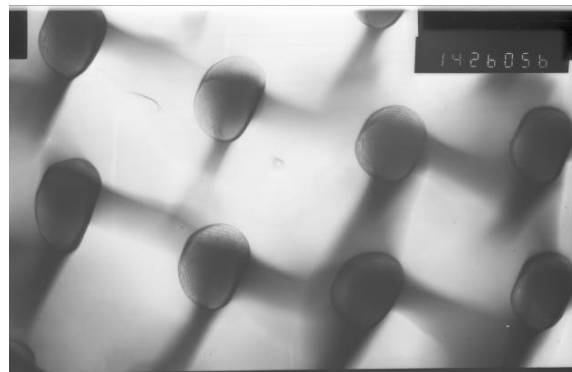
2.1.5. Influence of the composite materials composition on the peculiarities of phase interface formation

Microstructure investigations carried out during eutectics composition dependence in $\text{LaB}_6 - (\text{Ti}_x\text{Zr}_{1-x})\text{B}_2$ system on Ti/Zr ratio revealed that general trends of structure formation are observed throughout, while some differences are encountered only in the uniformity of reinforcing fibers diameters and in their distribution over the cross-section perpendicular to the growth direction. For the more thorough investigation of the interaction regularities on the phase interface samples for HRTEM were prepared according to the standard metallographic procedure. Thin platelets (0.2 mm) were cut from the rods perpendicular to their growth direction by means of electric discharge sawing (electroerosion cutting), that were further subjected to multi-step diamond polishing to the thickness of 20-40 μm , followed by ion milling. Unfortunately, the pronounced difference between the sputtering ratios of lanthanum hexaboride and zirconium - titanium solid solution diboride resulted in the pronounced difference in residual thickness of the sample after ion milling. In other words, after lanthanum hexaboride was almost fully etched away the residual thickness of the $(\text{Ti}_x\text{Zr}_{1-x})\text{B}_2$ phase was still too big for a high-quality HRTEM image formation. (Fig.17). No apparent influence of Ti/Zr ratio on the structure of the investigated materials has been established.

The investigation of samples was done Isabelle Jouanny, Mohamed Sennour, Marie-Hélène Berger (Centre des Matériaux Mines-ParisTech – ARMINES) and have received our group at 27.11.2010. Report we enclose.



$\text{LaB}_6 - (\text{Ti}_{0.6}\text{Zr}_{0.4})\text{B}_2$



$\text{LaB}_6 - (\text{Ti}_{0.4}\text{Zr}_{0.6})\text{B}_2$

Fig. 17. –TEM image of $\text{LaB}_6 - (\text{Ti}_x\text{Zr}_{1-x})\text{B}_2$ microstructure.

Moreover, from the images presented in Fig.17 the sufficient difference in lanthanum hexaboride and solid solution diboride phases thickness is clearly observed.

2.1.6. Main mechanical properties of $\text{LaB}_6\text{-(Ti}_x\text{Zr}_{1-x})\text{B}_2$ composites

As it has been mentioned above, mechanical properties of both LaB_6 and MeB_2 are considerably influenced by the direction of force application. This is also confirmed by the results of Young's modulus measurements of $\text{LaB}_6\text{-ZrB}_2$ composite grown on the single crystal LaB_6 substrates with different crystallographic orientation. Therefore, for better reproducibility of the results all investigated samples were grown using single crystal LaB_6 substrates with (001) plane oriented along the growth direction.

The investigation of chemical interaction influence on the phase interface on the composite failure it has been established that the most stable mechanical characteristic of the composites that is influenced only by stress and is completely reproducible for all samples is the Young's modulus. Moreover, the ultrasonic method of Young's modulus measurement chosen by the authors is a non-destructive technique, which gives the opportunity to use the same samples for other mechanical tests. Also, slight deviation of the samples composition from the strictly eutectic one and, therefore, the presence of small amounts of excess phases have no pronounced impact on the Young's modulus values. The use of Ti-Zr solid solutions diborides as the reinforcing phase in the investigated composites enabled to produce a series of samples with varying degree of lattice parameters mismatch and a somewhat varying internal stress in the composite resulting from the gradual lattice parameters and thermal coefficient change of the diboride phase (Ti-Zr solid solution diboride) in interrelation with Ti/Zr ratio. Unfortunately, the existing investigative techniques do not allow to single out the influence of these two factors on the mechanical properties of the composites under investigation. Young's modulus measurements were performed both on the samples produced from the high-purity starting components and from commercial powders. Low sensitivity of the chosen investigation method to the slight deviations of chemical composition and resulting inclusions of the excess phases enabled us to elucidate the $\text{LaB}_6\text{-(Ti}_x\text{Zr}_{1-x})\text{B}_2$ composite Young's modulus dependence from Ti/Zr ratio (Fig.18) even before the exact eutectic composition in these alloys has been determined.

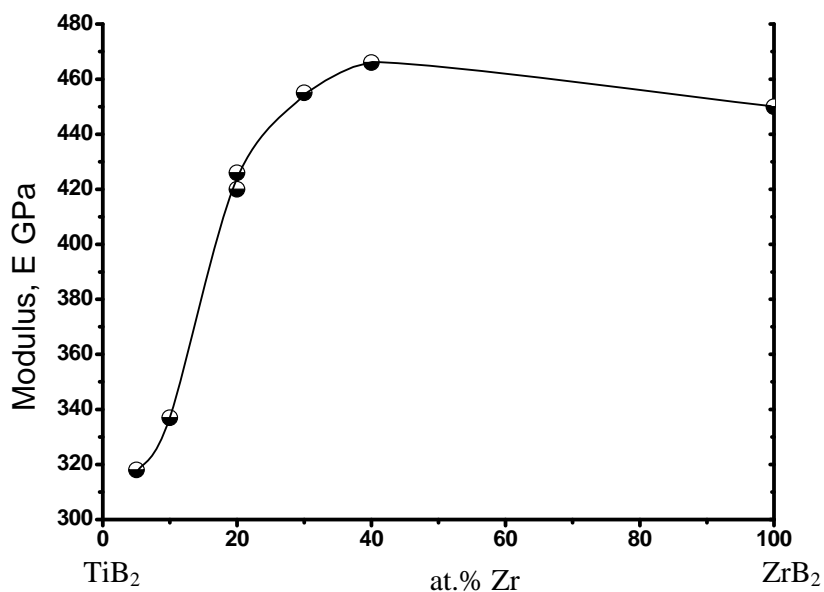


Fig. 18. – Concentrational dependence of Young's modulus in $\text{LaB}_6\text{-(Ti}_x\text{Zr}_{1-x})\text{B}_2$ composites.

As it has been predicted on the early stages of the present work, the semi-coherence of lattices on the phase interface has the crucial impact on structure formation processes and, as a result, on structure-sensitive mechanical properties of the composite. It should be specifically noted that the maximal value of Young's modulus has been measured for the $\text{LaB}_6\text{-(Ti}_{0.6}\text{Zr}_{0.4})\text{B}_2$ composition which, in turn, corresponds to the highest degree of eutectic structure homogeneity.

Investigations of bending strength and fracture toughness did not reveal any clear relation with the composite composition due to extreme sensitivity of these characteristics to even slight deviations from the eutectic composition and to impurities. However, we have discovered the principal change in the failure mechanism of the composite precisely for the $\text{LaB}_6\text{-(Ti}_{0.6}\text{Zr}_{0.4})\text{B}_2$ composition. That composition has the highest degree of lattice coherence of the constituents of the composite, which promotes crack propagation across the phase interface (Fig.19).

During fracture toughness measurements on the samples with matrix phase orientation (001) along the growth direction primary crack propagation occurred perpendicular to the load application direction (Fig.20).

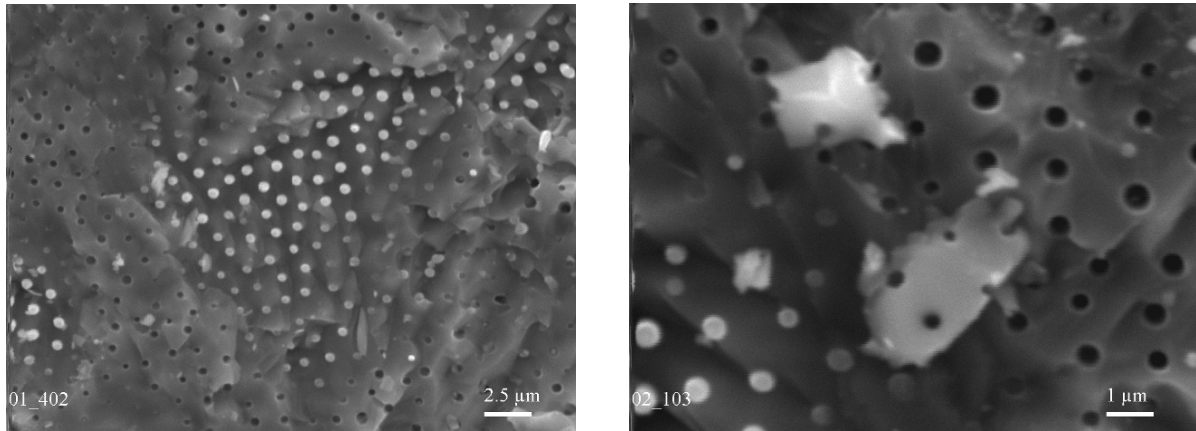


Fig. 19. – SEM image of the fracture surface after bending tests of $\text{LaB}_6\text{-(Ti}_{0.6}\text{Zr}_{0.4})\text{B}_2$ composition

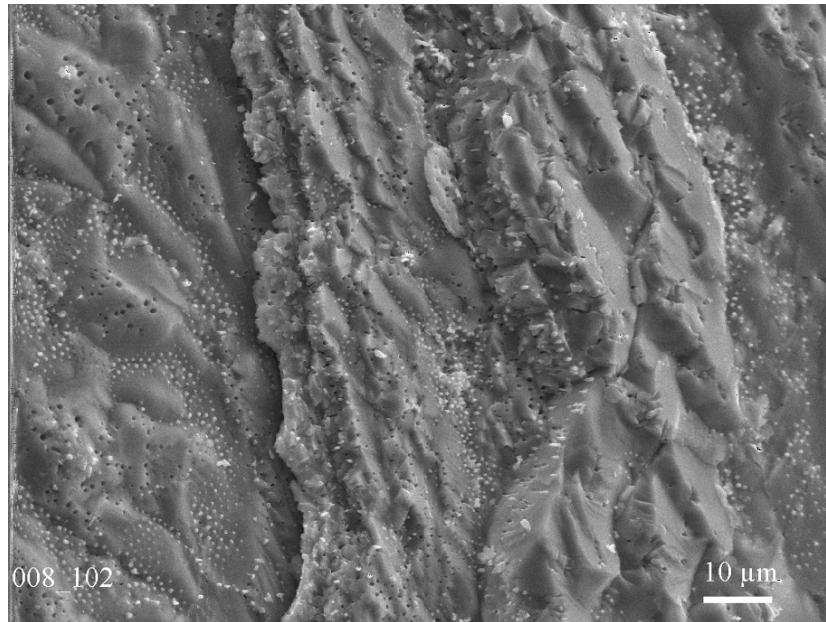


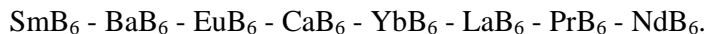
Fig. 20. – SEM image of the fracture surface after fracture toughness tests of $\text{LaB}_6\text{-(Ti}_{0.6}\text{Zr}_{0.4})\text{B}_2$ composition

2.2. Eutectic composition determination in $\text{SmB}_6 - (\text{Ti}_x\text{Zr}_{1-x})\text{B}_2$ system subject to x

It is a well known fact that metal-boron compounds are characterized by high interatomic bonding strength, low capability of internal stress relaxation and, as a result, these materials are considered as highly brittle [28]. On the other hand, isomorphic materials of this type differ in regard of the thermal shock resistance, abrasive capacity, and laser beam and ion irradiation failure resistance, which results from their different microplasticity (microbrittleness) and relaxation ability.

In order to evaluate the microplasticity (microbrittleness) in the series of isomorphic hexaborides produced by zone melting we have plotted a number of statistical curves that show the relation between the number of indentations with catastrophic failure (cracking) after fracture toughness indentation tests and the applied load [29]. We also calculated the value of work necessary for materials deformation during indentation formation which, according to [30] can be considered as “toughness”.

According to the obtained results the investigated compounds were ranged in the descending order of fracture toughness, i.e., in the descending order of deformation work of the material under indenter as follows:



This order is almost identical with another one that has been empirically established during another investigation concerning fracture and cleavage formation resistance of the same hexaborides (prepared by zone melting) using the visual estimation (analysis) of the TEM images of their fracture surfaces as well as by taking into account the relative changes of Me-Me bond lengths in the range of these compounds [31]. In this work it has been shown that the brittleness of MeB_6 type phases increases with the relative increase of Me-Me bond lengths (i.e., with the weakening of Me-Me bonds and, hence, with the increase of the relative contribution of B – B bonds).

The only exception is samarium hexaboride. The reason of its abnormal properties is caused by an unconventional effect described in [32, 33]. In these works a complex analysis of X-ray absorption L-spectra fine structure of Eu, Sm, and Yb in their hexaborides has been accomplished, which led to the conclusion that among the analyzed compounds only in SmB_6 samarium atoms simultaneously exist in two different valence states and are statistically distributed in crystallographically equivalent positions of the lattice. Recently [34], a direct evidence of samarium hexaboride “plasticization” has been obtained: during neutron diffraction analysis of phonon spectra of this compound an additional low-frequency mode has been discovered, which is the evidence of lattice softening in this compound as compared with other RE hexaborides with integer-valued valence. This means that in such a material stress (resulting from thermal effects, impurities and other factors during crystallization and crystal growth) relaxation occurs not via the dislocation mechanism but due to intrinsic elasticity. Investigations of pressure influence on samarium hexaboride structure [35] it has been shown that its lattice is about 20 % less rigid than for the cerium subgroup metals hexaborides where metallic ions have integer-valued valence (independent of valence value of 2 or 3). Investigation of high pressure (0-10 GPa) influence on structure modification (alteration) of integer-valued valence (CeB_6) and mixed valence (SmB_6) compounds has been carried out in [36]. Also, lattice parameters alteration under high pressure at room temperature were studied, and values of bulk modulus of elasticity were calculated.

The obtained results indicate that for samarium hexaboride, unlike other RE hexaborides, bulk modulus of elasticity changes with the change of applied external pressure. It is assumed that under external pressure up to 5 GPa its lattice deformation is facilitated due to samarium ionic radius diminishing with valence change without any increase of spatial filling density of its lattice. Under pressures higher than 6 GPa lattice compression followed by spatial filling density increase is observed. Lattice parameters and valence measurements of samarium hexaboride after pressure relaxation (removal) show that both return to their initial values. Due to such unique properties samarium hexaboride can undergo higher degree of deformation without catastrophic failure as compared with other RE hexaborides.

Taking into consideration the findings described above and considering the isostructurality of samarium and lanthanum hexaborides it is plausible to assume that it will be relatively easy to measure the magnitude of stress change in $\text{SmB}_6 - (\text{Ti}_x, \text{Zr}_{1-x})\text{B}_2$ system in interrelation with thermal expansion coefficients mismatch of the constituent phases: of samarium hexaboride and the reinforcing phase which is determined by Ti/Zr ratio in the solid solution diboride.

In order to verify this hypothesis a series of composite materials samples with a varying titanium and zirconium diboride ratio in the reinforcing phase with samarium hexaboride matrix phase has been produced by directional crystallization. Initially the samples of the $\text{SmB}_6 - (\text{Ti}_x, \text{Zr}_{1-x})\text{B}_2$ system were prepared with the volume fraction of the diboride phase equal to the one in the $\text{LaB}_6 - (\text{Ti}_x, \text{Zr}_{1-x})\text{B}_2$ system. However, consequent studies revealed that the non-monotonous character of the interrelation between the volume fraction of the reinforcing phase in Sm-based composite is much more pronounced than for the La-based systems. But even more interesting is our finding that in $\text{SmB}_6 - (\text{Ti}, \text{Zr})\text{B}_2$ system fundamental changes occur in the co-crystallization mechanism of the forming eutectic. During directional crystallization, contrary to the existing theory, in the case of $\text{SmB}_6 - (\text{Ti}, \text{Zr})\text{B}_2$ system the excess of titanium atoms in the diboride solid solution result in a prevailing tendency of platelet-like morphology formation for the reinforcing phase. For the system $\text{SmB}_6 - \text{ZrB}_2$ the reinforcing phase is formed exclusively with fiber morphology and the distribution of the fibers in the matrix is irregular (Fig. 21 a). For the $\text{SmB}_6 - (\text{Ti}_{0.2}, \text{Zr}_{0.8})\text{B}_2$ system the reinforcing phase still has the fiber morphology, however the forming fibers are arranged along some directions (Fig. 21 b). With the further increase of Ti content the reinforcing phase changes its morphology and the cross-section of the fibers becomes less equiaxed. When the Ti content exceeds 95 at % the fibers (reinforcing phase) are completely replaced by platelets (Fig. 21 d). Such observations contradict the existing concept which states that the minimal concentration of the reinforcing phase resulting in a platelet-like morphology must be in excess of 32 vol % which is almost 3 times higher than in the investigated system. Such abnormal behavior may be caused by some specific interaction between Sm and Ti atoms in case of phase interfaces orientation along specific crystallographic directions.

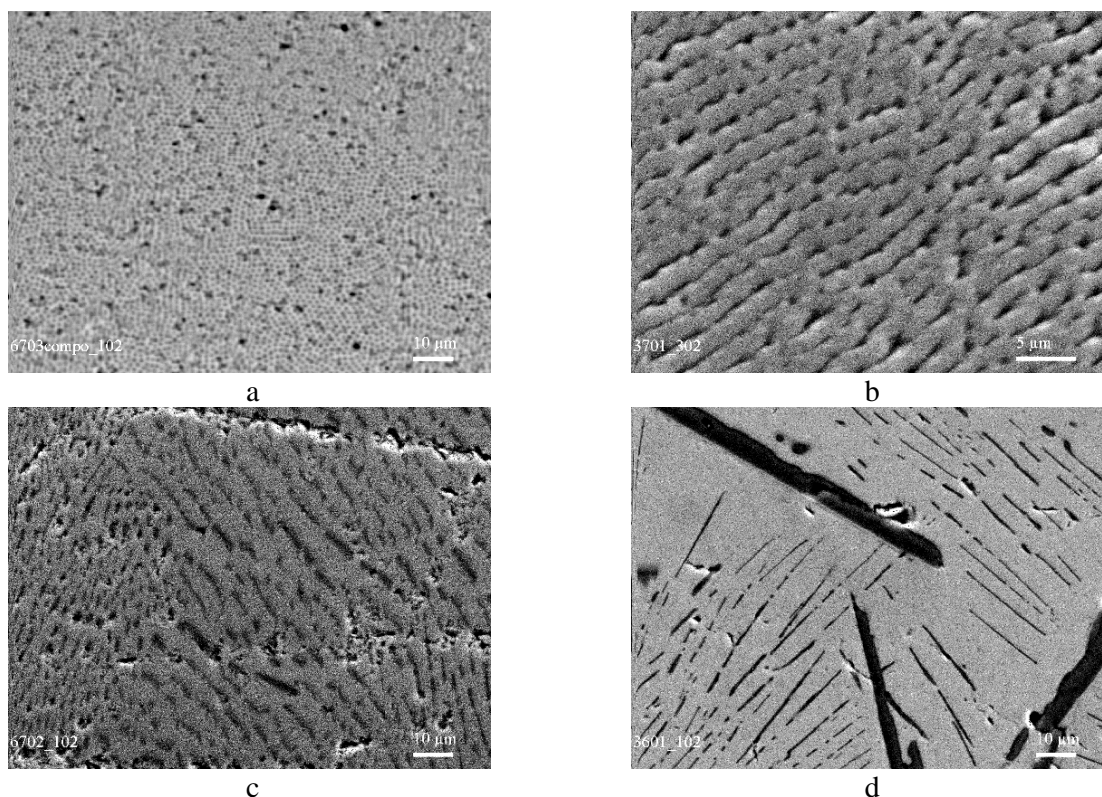


Fig.21. – Microstructure of a $\text{SmB}_6 - (\text{Ti}_x, \text{Zr}_{1-x})\text{B}_2$ directionally solidified eutectic composite,
a- $x=0$, b- $x=0,20$, c- $x=0,50$, d- $x=0,95$

It must be specifically noted that under conditions of reinforcing phase excessive concentration specific interaction on the phase interface also results in some changes of the particle shape (morphology) of the excessive diboride present in the $\text{SmB}_6 - (\text{Ti}_x\text{Zr}_{1-x})\text{B}_2$ composite structure (Fig. 22). For $x=0$ the particles are globular, for $x=0.4$ their shape evolves to rectangular, and for $x=0.8$ their shape becomes platelet-like. At the same time, for $\text{LaB}_6 - (\text{Ti}_x\text{Zr}_{1-x})\text{B}_2$ system the particle shape of the excessive diboride phase is globular for all valid x values (see Fig. 8 b).

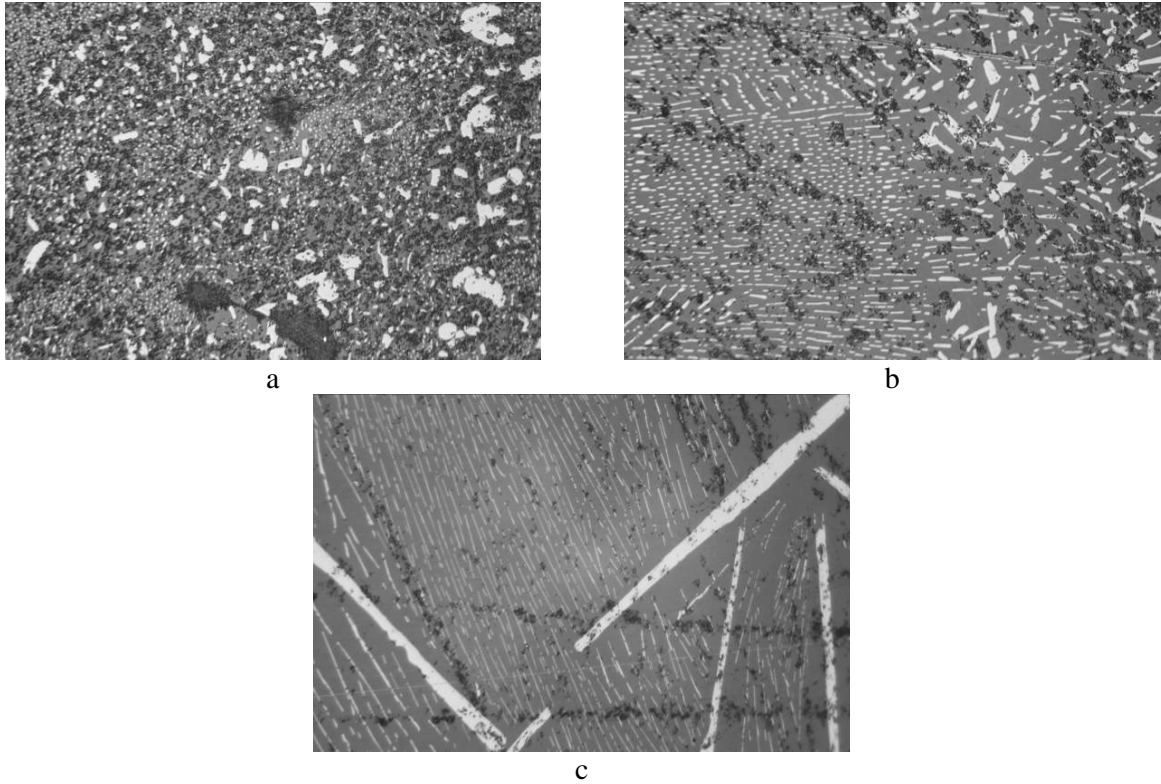


Fig.22. – Microstructure of a $\text{SmB}_6 - (\text{Ti}_x\text{Zr}_{1-x})\text{B}_2$ directionally solidified eutectic composite, **a-** $x=0$, **b-** $x=0,20$, **c-** $x=0,40$, **d-** $x=0,80$

These findings are of exceptional scientific importance for in-depth understanding and development of basic regularities of structure formation in eutectic materials.

CONCLUSIONS

It has been shown that co-orientation of crystalline phases is independent from matrix orientation for $\text{LaB}_6\text{-ZrB}_2$ system.

Ultrasonic and mechanical investigations have shown the influence of matrix orientation on composite elasticity modulus.

$\text{LaB}_6\text{-ZrB}_2$ DSE has been measured at 2000°C and was shown to exceed 200 MPa.

For the first time we have shown together with investigators of project P 273 that computer simulation results and experimental results are in good agreement for low crystallization rates ($0,5 \text{ mm/min} < v < 4 \text{ mm/min}$) and therefore it becomes possible to predict the increase of MeB_2 fiber diameter as a function of increasing crystallization rate.

The homogeneity of fiber distribution in the matrix phase and the uniformity of the fiber diameter are maximal when the Ti/Zr ratio in the diboride equals $3/2$ for $\text{LaB}_6\text{-(Ti,Zr)B}_2$ system, while the structure perfection is strongly influenced by the crystallographic orientation of the matrix. Stability of directional crystallization is minimal when the matrix orientation $[001]$ is parallel to the heat release direction.

Eutectic relations were determined for $\text{SmB}_6 - (\text{Ti}_x\text{Zr}_{1-x})\text{B}_2$ system (for $x=0; 0,20; 0,40; 0,60; 0,80; 0,95$). Also, in $\text{SmB}_6 - (\text{Ti,Zr})\text{B}_2$ system fundamental changes in the co-crystallization mechanism of the forming eutectic were observed during directional crystallization: contrary to the existing theory $\text{SmB}_6 - (\text{Ti,Zr})\text{B}_2$ system with the excess of titanium atoms in the diboride solid solution a tendency of platelet-like morphology formation is prevailing for the reinforcing phase.

Abnormally low heat conductivity of samarium hexaboride as compared to the one of lanthanum hexaboride was measured at temperatures higher than 1000°C .

The influence of thermal coefficient mismatch on stress inside the matrix phase in $\text{SmB}_6 - (\text{Ti,Zr})\text{B}_2$ systems with varying Ti/Zr is present but comparable with precision of measurement.

Results and findings obtained in the course of the present project realization were presented as 8 talks at 7 scientific conferences, and 2 articles were published in scientific journals.

BIBLIOGRAPHY

1. VB Filippov. Features of the origin and structure formation in directional solidification of the alloy $\text{LaB}_6\text{-ZrB}_2$ // Proceedings of International Conference HighMatTech, December 2007, Kiev, Ukraine, P. 146. (in Russian)
2. Filipov V.B., Paderno V.N., Lyashchenko A.B., Polovets S.E., Evdokimova A.V., Taran A.A., Peculiarities of structure and properties formation under conditions of directional crystallization of alloys in $\text{LaB}_6\text{-(Ti, Zr)B}_2$ system, Abstracts of 16th Int. Symp. on Boron, Borides and Related Materials, Sept. 2008, Matsue, Jpn. p. 130
3. Liashenko A., Polovets SE, Filippov VB, Paderno, VN, Taran A. Peculiarities of the structure and properties of directionally crystallized alloy $\text{LaB}_6\text{-(Ti, Zr) B}_2$, depending on the ratio of diborides titanium and zirconium Proceedings of the International Conference on Refractory Materials: Progress and problems ", 27-28 May 2008 Kiev, P.97 (in Russian)
4. V. Paderno, V. Filipov, E. Dickey. Effect of doping on phase interface condition and mechanical properties in $\text{LaB}_6\text{-ZrB}_2$ directionally crystallized alloys. Abstract of XVI International Conference on Solid Compounds of Transition Elements, 26-31 July 2008. Dresden. Germany, P.195
5. V. Filipov, A. Ievdokymova, A.Ljaschenko, V.Paderno Influence of Lattice Parameters Mismatch between Fibers and Matrix Phase on Structure and Properties of Directionally Solidified $\text{LaB}_6\text{ - (Ti,Zr)B}_2$ Composites, AFROS workshop on Aerospace Materials for Extreme Environments, June 3 – 5, Clayton (St. Louis) USA (2009).
6. E.Efimova, Y.Kartuzov, V.Kartuzov, B.Galanov, V.Filippov et al. Modeling of Structure Formation of Ceramic Fiber Boride Composite During Directed Crystallization of Eutectic Alloys, AFROS workshop on Aerospace Materials for Extreme Environments, June 3 – 5, Clayton (St. Louis) USA (2009).
7. V.Filipov, Distinctive Features of High-Temperature LaB_6 –Based Materials (Production and Properties), 3rd Directionally Solidified Eutectic Ceramics Workshop November 10-13, Seville, Spain (2009).
8. S.E. Polovets, V.N. Paderno, V.B. Filippov, A.B. Lyashchenko Structure and properties formation of composite materials in $\text{LaB}_6\text{-(Ti}_x\text{Zr}_{1-x})\text{B}_2$ system/ E-MRS 2009 Fall meeting, September 14-18, 2009, c.213 (2009)
9. H.Deng, E.C.Dickey, Y.Paderno, V.Paderno, V.Filippov. Interface Crystallography and Structure in $\text{LaB}_6\text{-ZrB}_2$ Directionally Solidified Eutectics // J.Am.Ceram.Soc., 90 (8), 2603-2609, 2007
10. B.A.Galanov, E.A.Efimova, V.B.Filippov et al. Modeling of Microstructure of $\text{LaB}_6\text{-ZrB}_2$ Eutectic Using Continuum Mechanics of Solidification Conditions, in Print

REFERENCES

1. R. Ashbrook, *J. Am. Ceram. Soc.*, **60**, (1977), 428.
2. Y. Waku, *KEY. ENG. MAT.*, **2**, (1999), 155.
3. A. Sayir, S. Farmer, P. Dickerson, and H. Yun, in Proceedings of Material Research Society Symposium. Warrendale, 1995. p. 21.
4. J. Y. Pastor, P. Poza, J. Llorca, J. I. Pena, R. I. Merino, and V. M. Orera, *Mater. Sci. Eng. A*, **308**, (2000), 241.
5. E. C. Dickey, V. P. Dravid, P. D. Nellist, D. J. Wallis, and S. J. Pennycook, *Acta Mater.*, **46**, (1998), 1801.
6. Y. Paderno, V. Paderno, V. Filippov, Y. Mil'man, and A. Martynenko, *Sov. Powd. Met.*, **31**, (1992), 700.
7. C. Chen, W. Zhou, L. Zhang, Z. Hao, Y. Jiang, and S. Yang, *Compos. Sci. Technol.*, **61**, (2001), 971.
8. Paderno Yu., Paderno V., Filippov B. Some peculiarities of structure formation in eutectic d- and f-transition metals diboride alloys // Boron-rich solids. AIF Conference proceedings № 231, Albuquerque, NM.- P.561-569.- 1990
9. Youri Paderno, Varvara Paderno, Vladimir Filippov, Crystal Chemistry of Eutectic Growth of d- and f-Transition Metals Boride // JJAP Series .-1994, 10.-190-193.- Japan Sci. Soc.,Tokyo
10. Paderno Yu., Paderno V., Filippov B. Some crystal chemistry relationships in eutectic cocrystallization of d- and f-transition metal borides // J. Alloys and Compounds.-**219**.- #1/2.-P. 116-118.-1995
11. H. Deng, E.C. Dickey, Y.Paderno, V. Paderno, V. Filippov. A. Sayir/ Crystallographic characterization and indentation mechanical properties of LaB₆-ZrB₂ directionally solidified eutectics // Journal of Materials Science, 39, c.5987-5994, 2004
12. Yu.Paderno, V.Paderno, V.Filippov, Some peculiarities Crystallization of LaB₆-(Ti, Zr)B₂ Alloys //J. Solid State Chemistry.-2000.-**154**.- 165-167
13. Kurz, P.R.Sahm, Gerichtet erstarrte eutectische Werkstoffe // Springer Verlag Berlin Heidelberg New York , 1975, 270 p.
14. JCPDS-International Centre for Diffraction Data. All rights reserved .1994
15. M.V. Mal'tsev, Radiography of metals, Metallurgizdat. M., 1952. 255 p. (in Russian)
16. I.I. Kornilov, "On the solid solutions of metallic compounds, Dokl AS USSR, 1951, **81**, P 597 (in Russian)
17. Glaser F., Ivanik W. The pseudo-binary system ZrB₂ - TiB₂ // Powder Met. Bull.- 1953.- **6**.- №4.- P. 126-132. (in Russian)
18. Transition Metal Diborides/ Post B., Glaser F., Moskowiz D. et all // Acta Metallurgica.- 1954.- **2**.- P. 20-26.
19. GA Meerson, GV Samsonov, RB Kotelnikov Some physico-chemical properties of borides of titanium and zirconium // Proceedings of the Physico-chemical analysis sector. IONKh USSR.- 1954.- **25**.- P. 89-93. (in Russian)
20. Vakuumnothermisch receive borides of refractory metals and study of some boride systems, GA Meerson, GV Samsonov, RB Kotelnikov et al - Sat Proceedings Mintsvetmetzolota .- M.: Metallurgizdat, 1955.- P. 209-225. (in Russian)
21. Wolfe BK Triple-metal phase in alloys .- M.: Metallurgy, 1964.- 222 p.
22. GV Samsonov and KI Portnoi Alloys based on refractory compounds .- M.: Oborongiz, 1961.- 304 p. (in Russian)
23. Particularly refractory elements and compounds. Handbook .- RB Kotelnikov et al, M.: Metallurgy, 1969.- 372 p. (in Russian)
24. Kieffer R., Benezovsky F. Solids .- Moscow: Metallurgiya, 1968 .- 384 p.
25. RB Kotelnikov. Technology of non-ferrous metals (Mintsvetmetzoloto) / Sat Nauchn. Proceedings .- 1958 .- vyp.29.- P. 339-348. (in Russian)
26. KI Portnoi, GV Samsonov Properties of ternary alloys titanium diboride, chromium and zirconium Dokl AS USSR.- 1957.- #116.- C. 976-978. (in Russian)

27. PI Loboda Anizotropiya mikrotverdosti napravleno-zakrystalizovanykh materialiv upon ocnovi hekcborydu lantanu // Physics himichna mehanika materialiv.- 1999, #3, P.93-101. (in Ukrainian)
28. GV Samsonov. Markovski LY, Zhigach A.F, Valyashko MG., Boron, Its Compounds and Alloys, Izd AS of Ukraine Kiev, 1960, 590 p. (in Russian)
29. Paderno V.N., Paderno Yu.B., Pilyankevich A.N., Lazorenko V.I. and Bulychyev. The micromechanical properties of melted borides of rare-earth metals. J. of the Less Common Metals, 1979, v.67, 431-436.
30. S.Palmqvist, Metod att bestamma segheten hos sproda material, Sazskilt hard metallar. Jernkont. Ann., 1957, v.141, #5, p.300-307.
31. Paderno YB, Pilyankevich AN, VN Paderno The electronic fractography hexaborides of alkali and rare earth metals, "Izv. AS of Ukraine. Inorganic Materials 1975 т.11, №5, с.856-858. (in Russian)
32. Vainshtein EE, Blokhin SM, Paderno Yu.B. X-Ray Spectral study of samarium hexaboride,. FSS. 1964 ,6, #10, P. 2909-2912. (in Russian)
33. Altshuler TS, Paderno Yu.B., Vinogradova OB Dudnik EM Electron paramagnetic resonance in samarium hexaboride, Technical Physics Letters, 1975, vol.1, no.19, P. 889-892.
34. Alekseev PA, Lazukov V., R. Osborn, Sadikov IP, Konovalova ES, Paderno Yu B., Rainford B. Magnetic excitations in the inelastic neutron scattering compounds with intermediate valence $\text{Sm}(\text{M})\text{B}_6$ (M - Ca, Ba, La). ZhETF, 108, № 3 (9), 1064-1080, 1995 (in Russian)
35. Effects of valence and intermediate valence on compressibility of the rare earth hexaborides / H.E.King, S.J.La Placa. T.Penney, Z.Fisk // Valence Fluctuations in Solids. - St. Barbara: North-Holland Publ. Co., 1981. - P. 333-336
36. ES Konovalova, TN Kolobyanina, Yu.B. Paderno, SI Lyukshia. Effect of pressure on the structure of samarium hexaboride, processing of materials at high pressures // Kiev, IPM IZdvo, 1987, P.88- 91 (in Russian)
37. Ashbrook R.I. Directional Solidified Ceramic Eutectics // J.Amer. Ceram.Soc. – 1960. - 9/10. – P.428-435

